## ABSTRACT

## NON-LINEAR DIGITAL CONTROL OF A MCKIBBEN MUSCLE SYSTEM

**by**
**Surinkumar Patel**

McKibben muscles are pneumatic actuators that have potential application in the rehabilitation of persons with physical impairments. These actuators have been known to exhibit similarities in human musculoskeletal systems. In order to better understand and improve the closed – loop control of these pneumatic muscles, a physical joint model was constructed with an agonist and an antagonist muscle operating under non-linear control. With the use of LabVIEW software, compliant McKibben air muscles and Flock-of-Birds sensor, the author was able to implement and compare a standard bang-bang controller and experimental non-linear digital Proportional (P) controller. The feedback mechanism is based on the input given from Flock-of-Birds sensor to achieve a desired position.

The results show the expected instability of the bang-bang controller, and confirm the superiority of the non-linear proportional method in achieving rapid and smooth movement of the joint from one target position to the next.

# NON-LINEAR DIGITAL CONTROL OF A MCKIBBEN MUSCLE SYSTEM

by
**Surinkumar Patel**

**A Thesis**
**Submitted to the Faculty of**
**New Jersey Institute of Technology**
**in Partial Fulfillment of the Requirements for the Degree of**
**Master of Science in Biomedical Engineering**

**Department of Biomedical Engineering**

**May 2005**

## APPROVAL PAGE

## NON-LINEAR DIGITAL CONTROL OF A MCKIBBEN MUSCLE SYSTEM

**Surin Patel**

Dr. Richard A. Foulds, Thesis Advisor — Date
Associate Professor of Biomedical Engineering, NJIT

Dr. David Kristol, Committee Member — Date
Professor & Associate Chair of Biomedical Engineering, NJIT

Michael T. Bergen, Committee Member — Date
Adjunct Professor of Biomedical Engineering, NJIT
VA New Jersey Health Care System, East Orange, NJ

## BIOGRAPHICAL SKETCH

**Author:** Surinkumar Patel

**Degree:** Master of Science

**Date:** May 2005

**Undergraduate and Graduate Education:**

- Master of Science in Biomedical Engineering,
  New Jersey Institute of Technology, Newark, NJ, 2005

- Bachelor of Science in Electrical Engineering,
  B.V.M Engineering College, V.V.Nagar, Gujarat, India, 1999

**Major:** Biomedical Engineering

To my beloved family
and in honor of my father
Bhagubhai Patel

## ACKNOWLEDGMENT

I would like to express my deepest appreciation to Dr. Richard Foulds, who not only served as my research advisor, providing valuable and countless resources, insight, and intuition, but also constantly gave me support, encouragement, and reassurance. Special thanks are given to David Kristol and Michael Bergen for actively participating in my committee.

Many of my fellow graduate students in the Biomechanics Research Laboratory are deserving of recognition for their support. Special thanks go to the knowledgeable engineers at the National Instruments Inc. Company, who have shared their expertise and professionalism.

## TABLE OF CONTENTS

## TABLE OF CONTENTS
## (Continued)

## LIST OF TABLES

## LIST OF FIGURES

## LIST OF FIGURES
## (Continued)

# CHAPTER 1

# INTRODUCTION

## 1.1 Objective

The objective of this Master's thesis is to present a working model of a biologically inspired robotic joint utilizing agonist and antagonist McKibben muscles under the non-linear control of a digital feedback system. Proportional (P) control via non-linear pulse width modulation (PWM) techniques is proposed for optimum results.

The experimental approach as well as a conventional Bang-Bang control method were evaluated and different fixed perturbations were exhibited by the system. The data from the joint angle sensor used in this model were determined to provide adequate feedback for achieving integration with the McKibben air muscles. The control of air pressure to each muscle was established through the reading of the Flock-of-birds sensor.

The PWM is introduced to add as a powerful technique to control varying air flow via tri-state valves using digital outputs from the computer. For the Proportional (P) control method, the advantages of better performance and stability are measured over the Bang-Bang control method. A LabVIEW program is introduced to incorporate a non-linear digital proportional control.

## 1.2 Background Information

Robot motion has often been compared to human motion. Human actions consist of highly non-linear elements such as multiple degree of freedom joints, muscles, ligaments and sensory organs [21]. Furthermore, the system has kinematics and actuator

redundancies. Robot movement takes on a much simpler form, which incorporates a trajectory planner algorithm and position feedback control [2]. In an effort to better understand muscle activity, it is important to note how muscle activation occurs from a biological viewpoint. The smallest subunit that can be controlled is called a motor unit because it is innervated separately by a motor axon. Neurologically the motor unit consists of a synaptic junction in the ventral root of the spinal cord, a motor axon, and a motor end plate in the muscle fibers [1]. Under the control of the motor unit are as few as three muscle fibers or as many as 2000, depending on the fineness of the control required. A muscle fiber is about 100 μm in diameter and consists of fibrils about 1 μm in diameter. Fibrils in turn consists of filaments about 100 Å in diameter.

In the figure below, the darker and wider myosin protein bands are interlaced with the lighter and smaller actin protein bands. The space between them consists of a crossbridge structure, and it is here that the tension is created and shortening or lengthening takes place. The actin filaments are composed of two strands of protein that are woven together as one. The actin filaments are anchored to Z lines that make the boundaries of the functional unit of muscle contraction called the sarcomere. There are many sarcomeres in a muscle fiber and Z lines are continuous across muscle fibers [4].

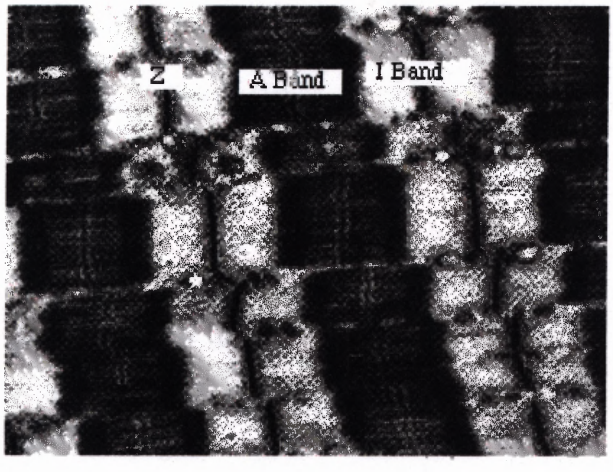


**Figure 1.1** A-Band, I-Band and Z line.

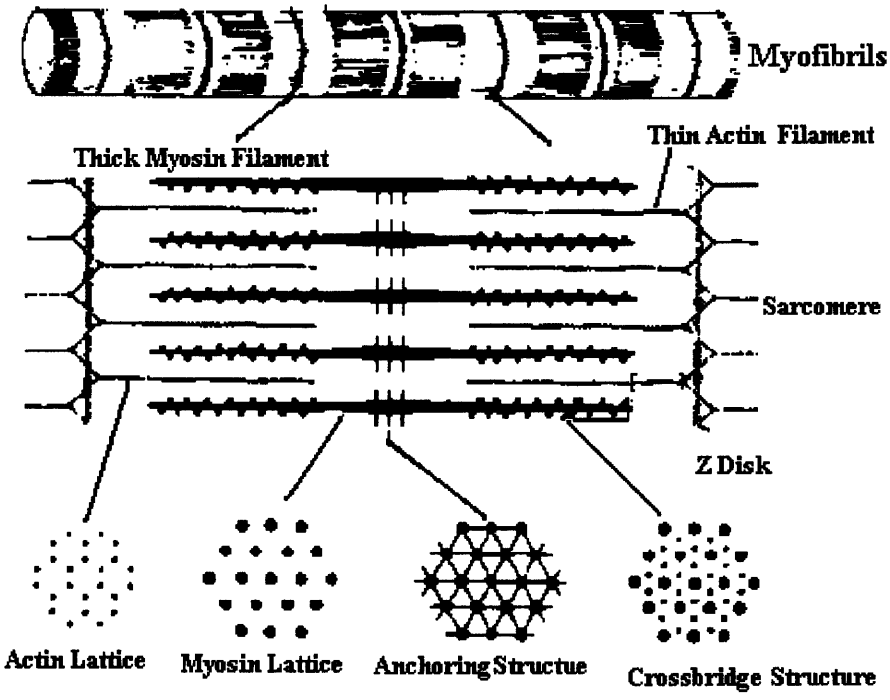


**Figure 1.2** Myofibril structure.

Muscle spindles are important proprioceptors. Muscle spindles are located within the belly of muscles and run in parallel with the main muscle fibers. The spindle senses muscle length and changes in length. It has sensory nerve terminals whose discharge rate increases as the sensory ending is stretched. This nerve terminal is known as the annulospiral ending, so named because it is composed of a set of rings in a spiral configuration. These terminals are wrapped around specialized muscle fibers that belongs to the muscle spindle (Intrafusal Fibers) and are quite separate from the fibers that make up the bulk of the muscle (Extrafusal Fibers) [3]. Stretching a spindle fiber initiates a volley of impulses in the sensory neuron (called an "I-a" neuron) attached to it. This I-a neuron contains velocity information. The impulses travel along the sensory axon to the spinal cord where they form several kinds of synapses.

Some of the branches of the I-a axons synapse directly with alpha motor neurons. These carry impulses back to the same muscle causing it to contract in a reflex loop.

Some of the branches of the I-a axons synapse with inhibitory interneurons in the spinal cord. These, in turn, synapse with motor neurons leading back to the antagonistic muscle, otherwise known as flexor. By inhibiting the flexor, these interneurons aid contraction of the extensor, or the agonist. Still other branches of the I-a axons synapse with interneurons leading to brain centers, e.g., the cerebellum that coordinates body movements.

Skeletal muscle makes up most of the body's muscle and does not contract without nervous stimulation [1]. During contraction, the myosin thick filaments attach to the actin thin filaments by forming crossbridges. The thick filaments pull the thin filaments past them, making the sarcomere shorter. In a muscle fiber, the signal for contraction is synchronized over the entire fiber so that all of the myofibrils that make up the sarcomere shorten simultaneously [4]. There are two structures in the grooves of each thin filament that enable the thin filaments to slide along the thick ones: a long rod-like protein called tropomyosin and a shorter bread-like protein complex called troponin. Troponin and tropomyosin are the molecular switches that control the interaction of actin and myosin during contraction.

In order to better understand and replicate the complex control of the central nervous system (CNS), investigation was required into several musculoskeletal systems models that biomedical researchers developed. These systems are then transformed from highly non-linear into linear to give the ability to pursue a quantitative approach to investigate the CNS and the peripheral system. Although much consideration has been given to the individual components of these systems, little research has examined their contribution to system as a whole. From a control-engineering viewpoint, the author is only interested in the control of simple positioning tasks within single degree of freedom.

### 1.3 Summary

In this experiment, the physical model is constructed in a manner that minimizes the effect of non-linear properties. Examination of a single degree-of-freedom (DOF) movement, and limited range of motion enable optimization of feedback loops to achieve stability. A block diagram of the whole system is shown in Figure 1.3.

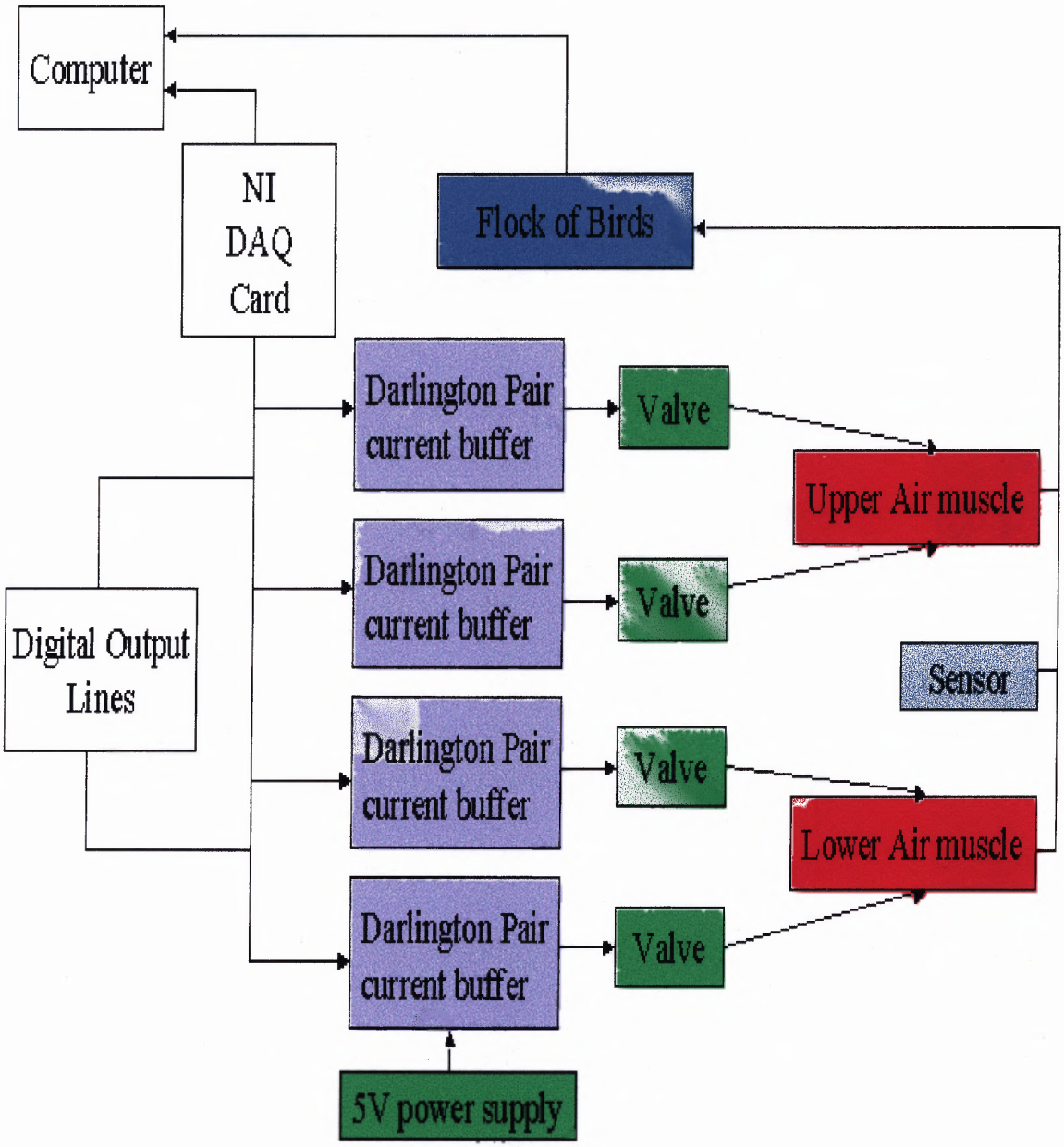


**Figure 1.3** Block diagram of whole system.

The apparatus includes a pair of McKibben pneumatic muscles connected in agonist/antagonist fashion about a single joint. The control of movement in this model requires co-activation of agonist and antagonist muscles. This is done by applying a force via one muscle to get the joint moving, and turning on the other muscle to act as a brake to slow the joint to achieve the desired angle. Although co-activation was previously executed through the Bang-Bang control method (23), further investigation was needed to increase the overall stability. Pulse width modulation technique used to produce proportional controller.

# CHAPTER 2

## COMPONENT INTEGRATION

Many elements were included in constructing this single joint air muscle model. The System includes two McKibben AM-02 air muscles and a 5 hp compressor to emulate agonist and antagonist muscle activation. The digital control of the air pressure to the two air muscles is accomplished by four Mead Fluid Dynamics isonic two-way solenoid valves, which were modified to three-way control in order to maintain position. Flock of Birds from the Ascension Technology Corporation (ATC) is used as a motion tracking system. The sensor of the FOB system is fixed at the wrist of the arm. The FOB simultaneously tracks the position and orientation of the sensor with respect to the transmitter.

The continuous streams of position data are captured for the feedback. The joint model also requires the use of four digital outputs to trigger the on/off state of the pneumatic valves. Control of the pneumatic valves was accomplished through the use of National Instruments (NI) LabVIEW software v.6i and a NI- DAQCard-AI-16E-4 data acquisition device. A custom current amplifying circuit interfaces the DAQCard to the valves. The power requirements were supplied by a separate continuous 5V DC amplifier. In this chapter, the joint model composition, component limitations and effects on stability are explored.

## 2.1 McKibben Air Muscles

The McKibben pneumatic artificial muscle was invented in 1950s by physician Joseph L. Mckibben to motorize pneumatic arm orthotics to help control disabled hands. The Bridgestone Rubber Company of Japan has commercialized them for robotic applications, and they were re-engineered by Prof. Jack Winters for construction of biomechanically realistic skeletal models [8]. The Air Muscle is an extraordinary actuator that is small, light and simple. It is soft, has no stiction, and is easily controllable and exceptionally powerful. The Air Muscle consists of a rubber tube covered in tough plastic netting, which shortens in length like a human muscle when inflated with compressed air at low pressure. Air Muscles are normally operated using compressed air in the 0-60psi (0-4 bar) range.

**Figure 2.1** McKibben air muscle.

Several companies (Shadow, Images SI, Kinetic Muscle Inc) market a variety of sizes of air muscles [9]. Many users fabricate custom versions, as they are quite simple to construct. The one, which used in this project is 20 mm in diameter and weight is approximately 10 grams. The Image SI Air Muscle is a simple yet powerful device for providing a pulling force. It behaves in a very similar way to a biological muscle. When actuated with a supply of compressed air, they contract by up to 40% of its original length. The force it provides decreases as it contracts, and the first few percent of the contraction are very powerful indeed.

**Air Muscle Construction**

The Core of an Air Muscle is a rubber tube....

**Figure 2.2** Core of air muscle.

...wrapped in a tough helical plastic weave....

**Figure 2.3** Air muscle plastic weave.

.... which shortens in a scissor action when pulled out, just like a Chinese finger puzzle.

As the rubber tube fills with air it is forced to expand. A small Air Muscle, at just 6mm in diameter, has the strength, speed and fine stroke of a finger muscle in a human hand [9]. An Air Muscle 30mm in diameter is capable of lifting more than 70 Kg at a pressure of only four bar, while a large muscle (50mm) has enough power to pull down a brick wall.

When the internal bladder is pressurized, it expands like a balloon and presses outward against the external plastic weave. The cylindrical shape of the inner tube allows helical weave to act as a pantograph and converts circumferential pressure forces into axial contraction force (Figure 2.4).

**Properties of Air Muscle**

The Air Muscle behaves in a different manner to the pneumatic cylinder or other actuator. As the Air Muscle contracts under constant pressure, pulling force produced between the endpoints decreases. The maximum possible force at a given pressure is obtained when the Air Muscle is pulled out as far as possible. If the Air Muscle is not taut, then it will not yield its full force [9]. At a constant pressure, the curve of the Force against Length is shown in Figure 2.4.

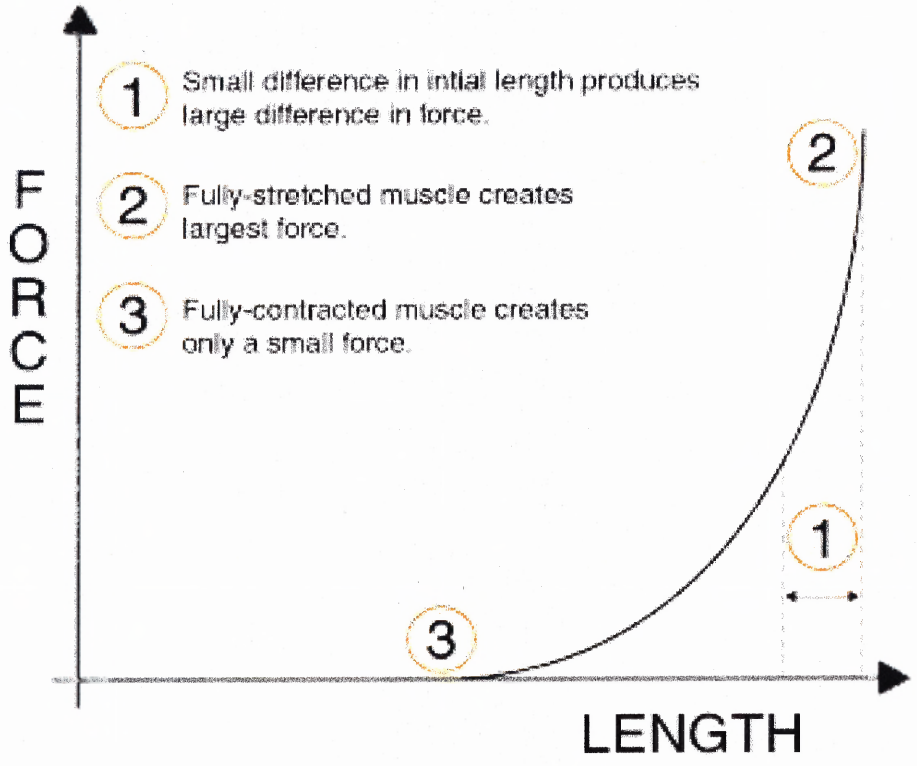


**Figure 2.4** Force-Length curve.

The relationships between tension, length, velocity and activation are major characteristics of actuators, which vary greatly from type to type. Human skeletal muscles also have its own particular characteristics: for example, the convex shape active tension-length relationship, the non-linear passive tension-length relationship, and the hyperbolic tension-velocity relationship. Each of these properties is also a function of activation level. The air muscles used in this experiment measure 210 mm in length. The diameter is 20 mm and the muscle can pull a load of 45 lbs. at the maximum 50psi pressure.

## 2.2 Flock of Birds Sensor

The motion tracking system, Flock of Birds sensor was invented by the company called Ascension Technology Corporation (ATC). The Flock of Birds (FOB) is a six degrees-of-freedom measuring device that can be configured to simultaneously track the

position and orientation of multiple sensors by a transmitter. Each sensor is capable of making up to 144 measurements per second of its position and orientation when the sensor is located within ± 4 feet of its transmitter. An optional extended range transmitter increases this operating range to ± 8 feet. The FOB works by transmitting a pulsed DC magnetic field that is simultaneously measured by all sensors in the Flock. From the measured magnetic field characteristics, each sensor independently computes its position and orientation and makes this information available to your host computer [11].

An FOB consists of one or more electronic units or extended range transmitter controllers interconnected via a Fast Bird Bus (FBB). To increase the Flock size, an additional Bird unit must be plugged into the FBB for each additional sensor. Because each bird attached to the bus has its own independent computer, the FOB can simultaneously track each sensor, providing up to 144 measurements per second from each. The Flock can be configured to track from one to four sensors simultaneously with one or more RS-232 interfaces to a host computer [10]. The actual physical components of the FOB used for this model is shown in Figure 2.5. The Table 2.1 gives the name of component corresponding to Figure 2.5.

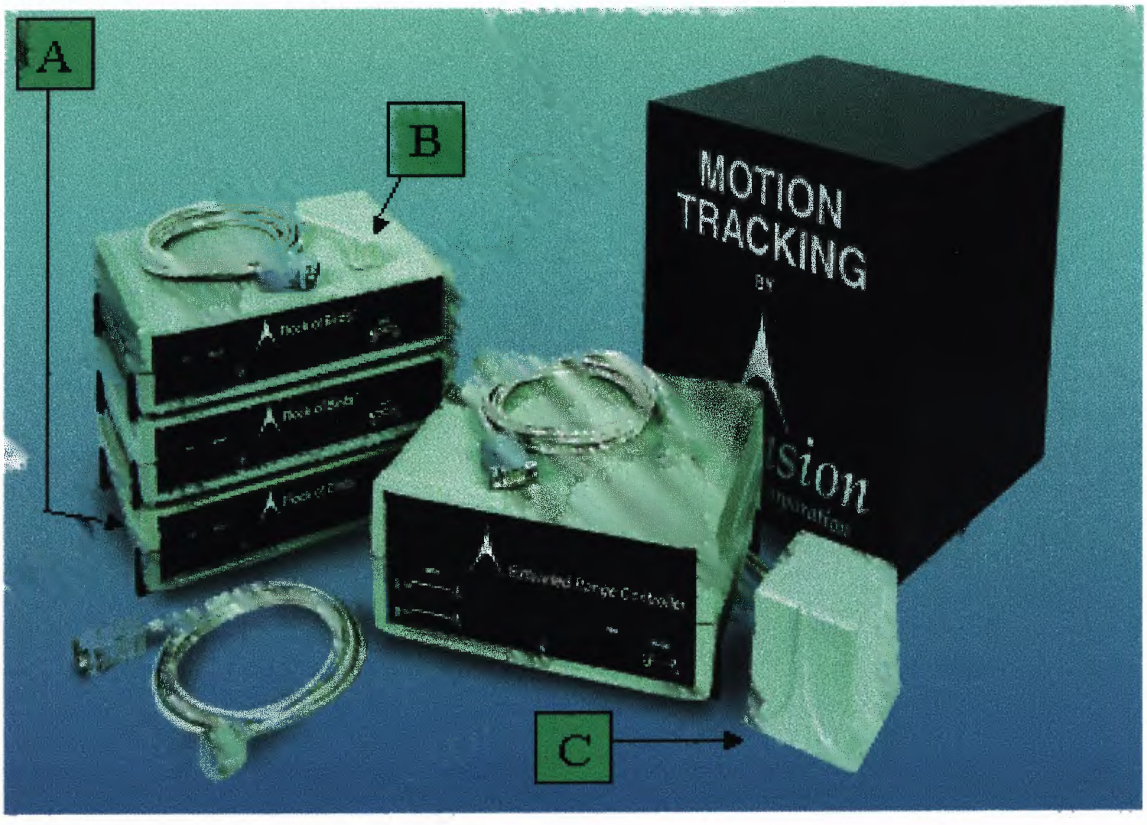


**Figure 2.5** Flock of Birds sensor.
Source: Ascension Technology Corporation.

**Table 2.1** Components of Flock of Birds Sensor

| Notation in Figure 2.5 | Component |
|---|---|
| A | Electronics Unit |
| B | Bird Sensor |
| C | Transmitter |

Each Bird unit in the Flock contains two independent serial interfaces. The first interface is for communications between the host computer and the FOBs. We may configure this interface as a full duplex RS-232C interface or a half duplex RS422/485 interface. The second interface is a dedicated RS 485 interface for communications between the flock members. The user and intra-flock RS422/485 buses are generally

called the Fast Bird Bus. The host computer may utilize either a single or multiple RS232/422/485 interfaces to command and receive data from all Bird units. The host can send commands and receive data from any individual Bird unit because each Bird unit is assigned a unique address on the FBB via back-panel dipswitches [11]. The FOBs can be configured to suit many different applications - from standalone unit with a single transmitter and sensor to more complex configurations consisting of various combinations of transmitters and sensors. The Figure 2.6 below shows the block diagram of the standalone Flock of Birds configuration set up, a single Bird unit with its own transmitter and sensor using the RS232 interfaces, used for this thesis.

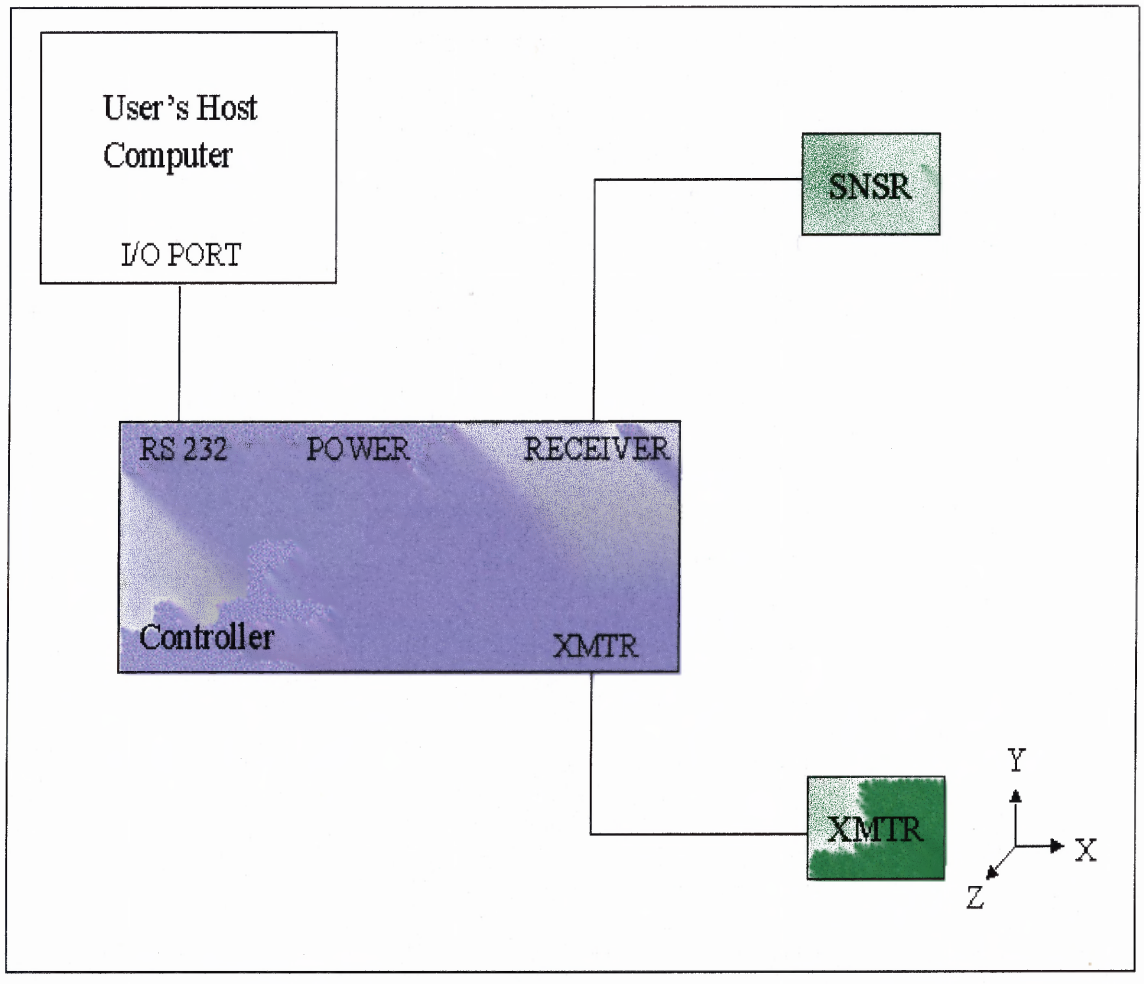


**Figure 2.6** FOB set up for single Bird sensor interface to host computer.

The main important precaution we have to take is the location of electronics controller unit, transmitter and Bird sensor. Generally, the electronics controller unit is not located on top of or under other electronic equipment that is not shielded. The transmitter should be mounted on a non-metallic surface such as wood or plastic, using non-metallic bolts or 300 series stainless steel bolts. It also may be mounted on the top front edge of the electronics controller unit. Do not mount the transmitter on the floor (concrete included), ceiling, or walls because these all contain metal or may have large metal objects directly on their opposite side. Because the transmitter generates magnetic fields, it may interfere with computer's display, causing image bending, jitter or color distortion. The Bird sensor should also be mounted on a non-metallic surface as wood or plastic. It should not be located near power cords, power supplies, or other low-frequency current-generating devices. Their emanations will be picked up by the sensor and converted into noise on the output position and orientation measurements [11].

In this thesis, the Bird is operated in the Normal Addressing mode. On the back panel of each Bird unit there is a dipswitch that must be set to select the baud rate, unit address, and other functions. Whenever you change the dipswitch settings, you must toggle the Bird's FLY/STDBY switch to STDBY and then back to FLY for new setting to be recognized by the system. The technical and physical specifications of FOB unit are introduced in Appendix A. The Dipswitch Settings for the normal address mode is shown in Appendix B.

The Dipswitches settings, which are used particular for this model setup is shown in the Table 2.2.

**Table 2.2** Dipswitch Settings of Flock of Birds Sensor

| *Dip Switch* | *1* | *2* | *3* | *4* | *5* | *6* | *7* | *8* |
|---|---|---|---|---|---|---|---|---|
| *Setting (ON/OFF)* | *ON* | *ON* | *ON* | *OFF* | *OFF* | *OFF* | *OFF* | *OFF* |

## 2.3 Transistor Circuit

A digital input/output (I/O) block is used to transmit the signal to the four solenoid valves. In order to accomplish this task, four digital lines must transmit a signal from the computer to activate a high logic "one" state or a low logic "zero" state [12]. The digital values are produced by a LabVIEW program. The digital I/O circuit includes N-P-N transistors, different value resisters and ½ watt diodes to provide a means of switching current to the valves since the data acquisition (DAQ) card does not produce sufficient output current. The current draw required to turn the valves is 263mA, which discussed in next section. The Figure 2.7 shows the connection on the transistor power amplifier circuit board.


**Figure 2.7** Transistor power amplifier circuit board.

The transistor driver subsystem is an electronic switch. The output signal from the transistor has a much larger current than that of the input signal up to 100mA. The transistor driver circuit uses an NPN transistor, which has three legs known as the **base**, **emitter** and **collector**. The Figure 2.8 shows the schematic diagram of the transistor, which is used in this thesis. The job of the transistor is to allow the small amount of current that enters its 'base' terminal to control the amount of current flowing from its 'collector' terminal to its 'emitter' terminal [15]. When the voltage between the base and the emitter is at least 700mV, a small current flowing into the base will cause a much larger current to flow from collector to the emitter.

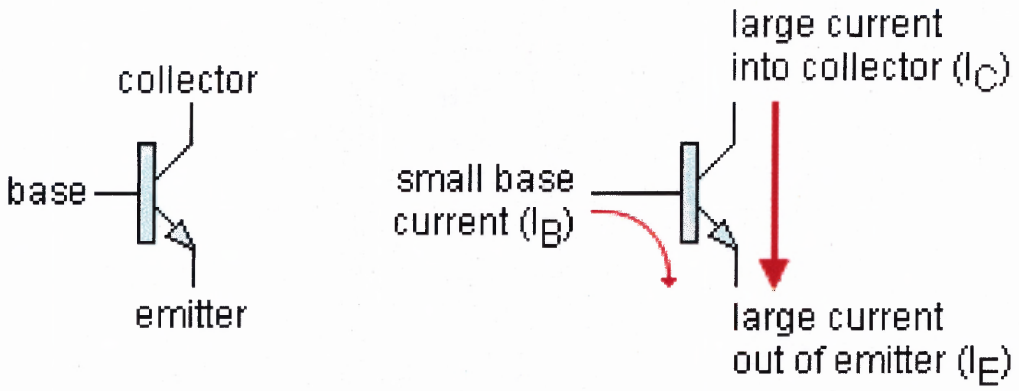


**Figure 2.8** Motorola P2N2222A transistor.

The transistor gain can be calculated as follows:

$$\text{gain } (h_{FE}) = \frac{\text{collector current}}{\text{base current}} = \frac{I_C}{I_B}$$

Junction transistors consist of two junctions made from N-type and p-type semiconductor materials and are called bipolar transistor. Motorola P2N2222A silicon transistors were used to switch (on/off) the valve status and amplify the current requirement [13]. A single transistor arrangement in the circuit lacks the gain to drive the pneumatic valve. The Darlington Pair driver subsystem provides an output signal that is powerful enough to drive high power output subsystems. A Darlington Pair is needed to amplify the current and this is achieved by the first transistor's emitter feeding into the base of the second transistor providing the two transistor's collector terminals short circuited. The Figure 2.9 shows the schematic diagram of the Darlington Pair arrangement of the transistor. The total gain can be calculated by multiplying the gain of each transistor together. Similarly, the trigger voltage at the base doubles from 0.7V for one transistor to 1.4V for two transistors.

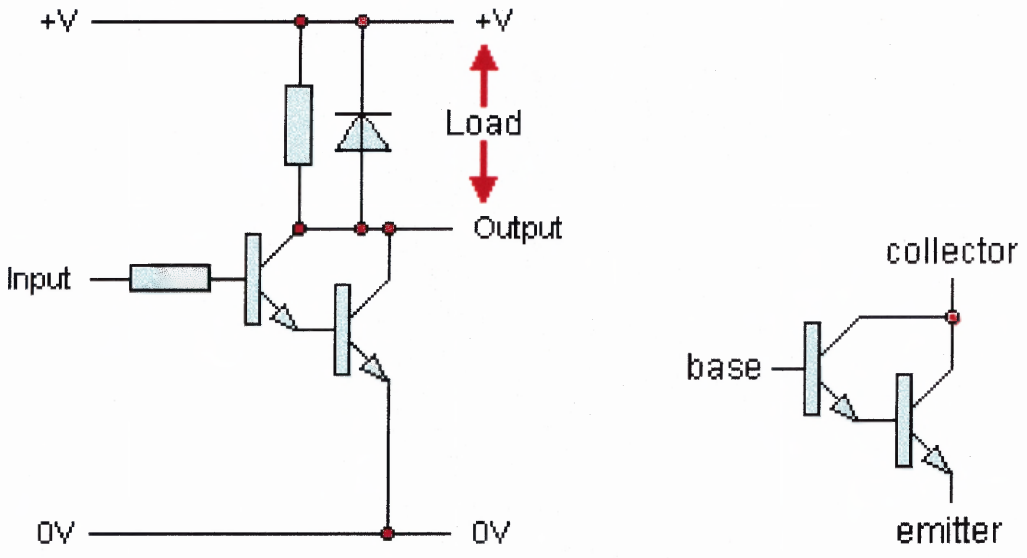


**Figure 2.9** Darlington pair arrangement of transistors.

## 2.4 Mead Fluid Dynamics Valves

The Isonic solenoid valves used in the model contains an integrated electronics board with surge suppression and an LED. Mead's patented "half-shell" design of the three-way valves allows flow channels and component compartments to be designed directly into the body. The body halves are joined by ultrasonic welding, creating a strong bond and hermetic seal [14]. The unique Isonic manifold allows instant valve connection and removal, without the aid of a tool. An exploded view diagram of the Mead Isonic valve is provided in the Figure 2.10.

The three-way design incorporates an inlet port, outlet port and hold. The valves have been modified to facilitate individual flow control patterns by implementing a three-way design. This was accomplished by sealing the exhaust port of the 2$^{nd}$ valve in the airflow path from the air compressor to the air muscle. The input port of the 1st valve is connected to the manifold. The output port of 1$^{st}$ valve connects to the input port of the 2$^{nd}$ valve, and the output port of the 2$^{nd}$ valve is connected to the air muscle.

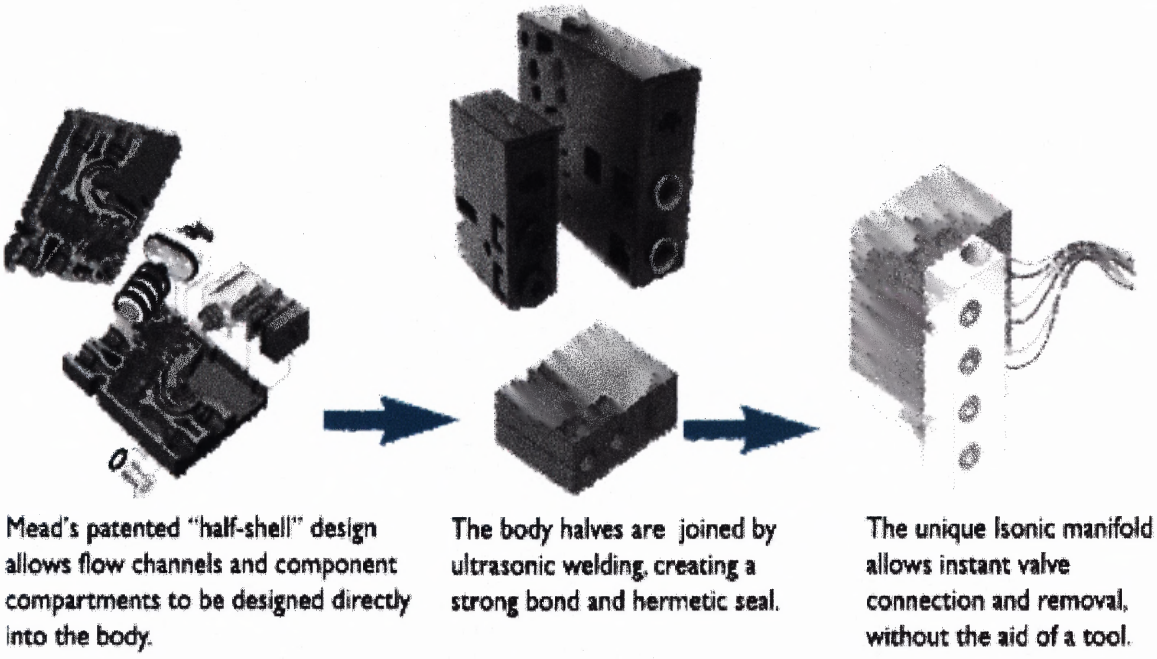


**Figure 2.10** Mead Fluid Dynamics solenoid three-way valve.
Source: Mead Fluid Dynamics Inc.

The flow control patterns relating to the control of air pressure into each air muscle can be seen in Table 2.3.

**Table 2.3** Flow Control Patterns of a Single Air Muscle using a 3-way Design

| *Sequence* | *Valve 1* | *Valve 2* | *McKibben Air Muscle* |
|---|---|---|---|
| *1* | *on* | *on* | *Air flows in up to max pressure, contracts* |
| *2* | *off* | *on* | *Air flows out of Valve 1 & 2, releases* |
| *3* | *on* | *off* | *Air flows into valve 1, holds contracted* |
| *4* | *off* | *off* | *Air flows out of valve 1, holds contracted* |

The electrical characteristics of the solenoid valves play an important role in developing the transistor circuit [14]. The circuit was build to amplify the current supply needed to actuate the valves. Using a multimeter, the resistances of the valves were

\measured to be 19 ohms. The current draw required to turn on the valves was then calculated using Ohm's Law:

$$E = I \times R$$

$$I = 5V / 19ohms$$

$$I = 263mA$$

Therefore, the circuit was built so that the transistors are capable of switching the minimum 263mA current rating. The transistor's maximum collector current (Ic) rated 600mA as a result of the overall 100 gain rating achieved through the Darlington Pair arrangement. The total gain can be calculated by multiplying the gain of each transistor together [13]:

$$\mathbf{h_{FE} = T_1\, h_{FE} \times T_2\, h_{FE}}$$

From this, calculations can be made for both first and second of the transistor's base currents ($I_{B1}$ & $I_{B2}$, respectively) to switch the 263mA minimum collector current using the following equations:

$$\text{First transistor Gain} = IC1 / IB1 = 10$$

$$IB1 = 26.3mA / 10$$

$$IB1 = 2.63mA$$

$$\text{Second transistor Gain} = IC2 / IB2 = 10$$

$$IB2 = 263mA / 10$$

$$IB2 = 26.3mA$$

The Darlington Pair circuit is then repeated four times for the activation of the four valves into the buffer circuit. Only one of the four duplicate Darlington Pair arrangements is shown in Figure 2.11.

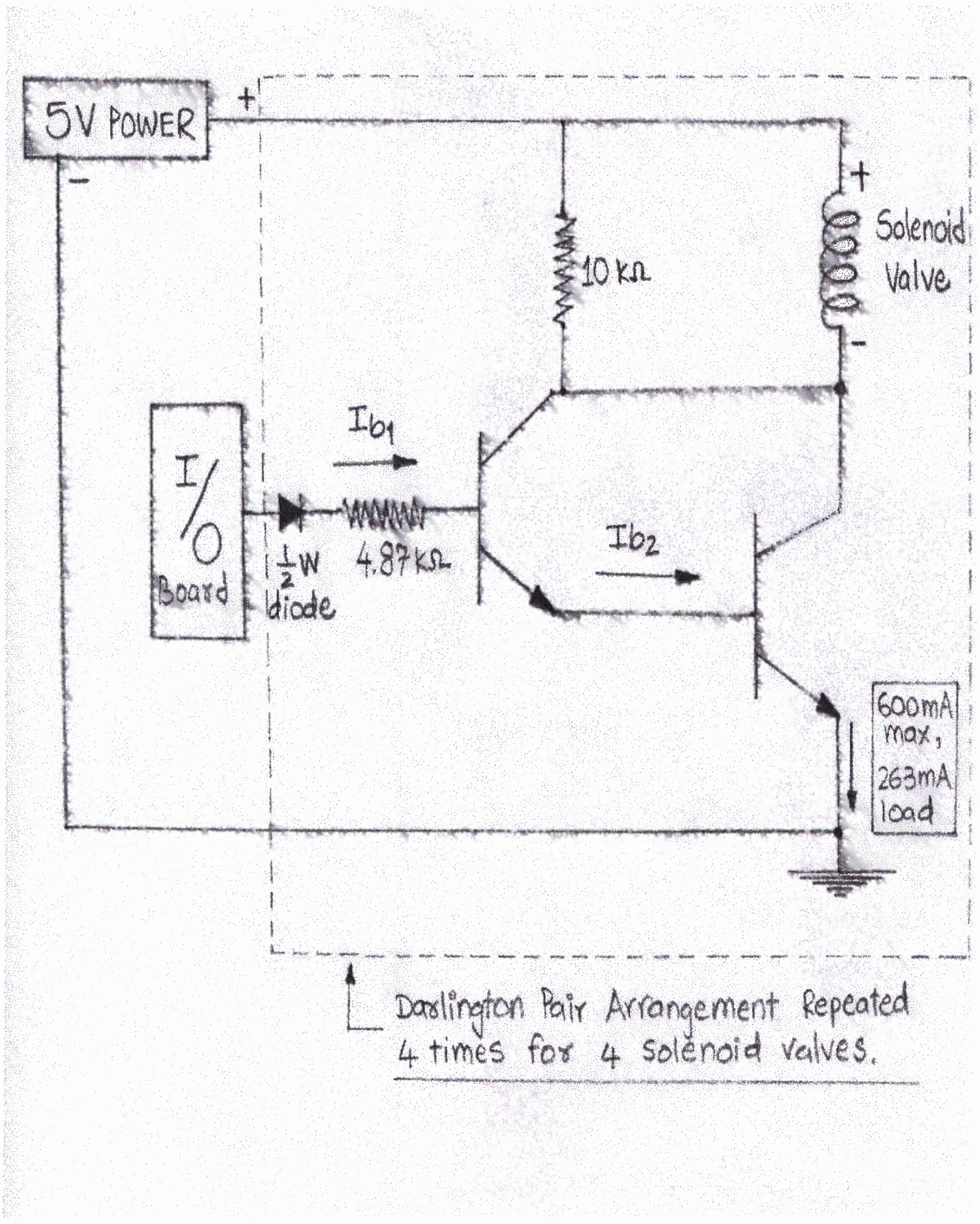


**Figure 2.11** Circuit diagram for darlington pair arrangement.

## 2.5 Data Acquisition Card

The software used to control the model was written in National Instruments (NI) LabVIEW v.6i. In order to read data from Flock of Birds sensor via serial port and activate the pneumatic valves, a data acquisition system was needed for program control. The DAQCard E Series cards are multifunction analog, digital and timing I/O cards for computers equipped with PCI slots [16]. The card that was selected, National Instruments PCI-6024E is a low-cost data acquisition board that uses E Series technology to deliver high-performance, reliable data acquisition capabilities in a wide range of applications. We get up to 200 kS/s sampling and 12-bit resolution on 16 single-ended analog inputs. It also features with two 12-bit analog outputs, 8 lines of TTL-compatible digital I/O, two 24-bit counter/timers for timing I/O. The PCI-6024E multifunction data acquisition board is shown in the below Figure 2.12 [18].

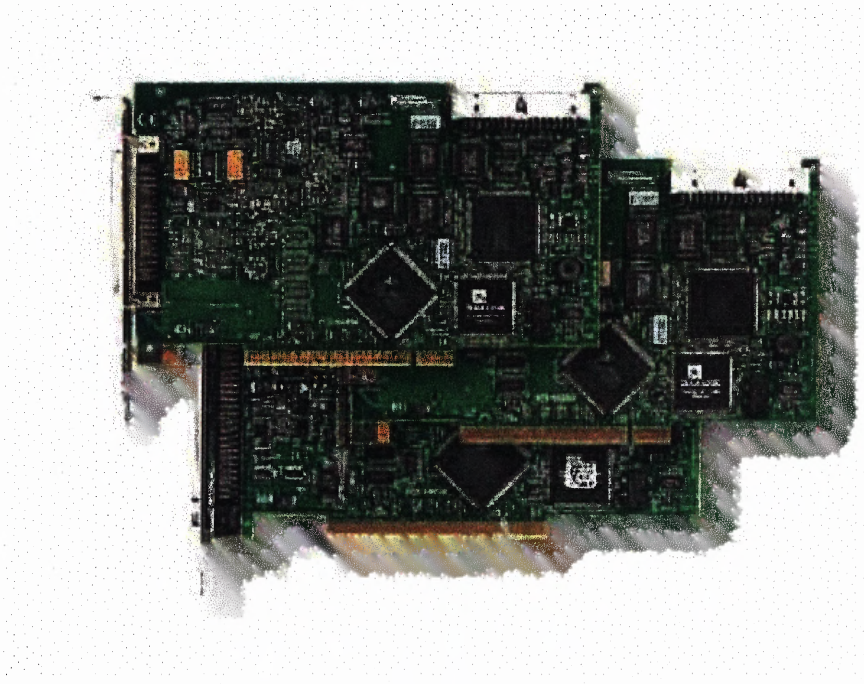

**Figure 2.12** NI PCI-6024E.
Source: National Instruments (NI) Corporation.

LabVIEW and LabWindows/CVI are program development software packages for data acquisition and control applications. LabVIEW uses graphical programming, whereas LabWindows/CVI enhances traditional programming languages. Both packages include extensive libraries for data acquisition, instrument control, data analysis and graphical data presentation. LabVIEW features interactive graphics, a state-of-the-art user interface, and a powerful graphical programming language. The LabVIEW Data Acquisition VI Library, a series of VIs for using LabVIEW with National Instruments DAQ hardware, is included with LabVIEW [16].

NI-DAQ has both high-level DAQ I/O functions for maximum ease of use and low-level DAQ I/O functions for maximum flexibility and performance. Examples of high-level functions are streaming data to disk or acquiring a certain number of data points. An example of a low-level function is writing directly to registers on the DAQ device. NI-DAQ does not sacrifice the performance of National Instruments DAQ devices because it allows multiple devices operate at their peak performance. NI-DAQ also internally addresses many of the complex issues between the computer and the DAQ hardware such as programming interrupts. NI-DAQ maintains a consistent software interface among its different versions to decrease code modifications. In this model, we are using four out of eight digital I/O lines for activation of the four mead fluid dynamic valves [16].

## 2.6 I/O Connector Block

The I/O connector block used for the DAQCard E Series cards has 68 pin connections. It is referred to as the CB-68LP [17]. The connector block includes standoff feet for use on a desktop or mounted in a custom panel. The CB-68LP has a vertical mounted 68-pin

connector. The arrangement and details of the I/O board pin connections can be found in Appendix E. It is important to note that exceeding the maximum input voltage rating can damage the DAQ E Series card and other connected hardware. The connections which are made with CB-68LP are shown in the Figure 2.13.

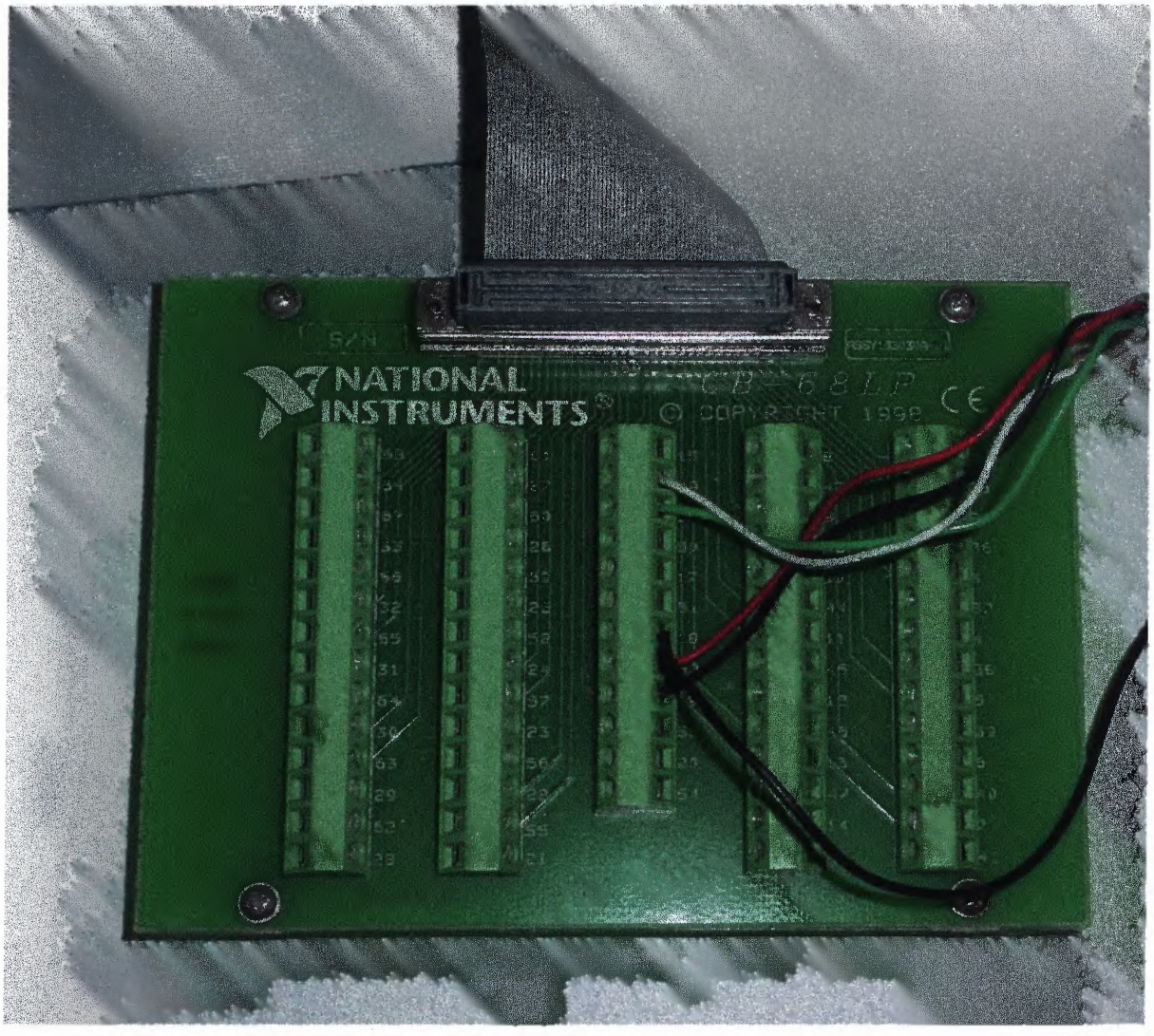


**Figure 2.13** CB-68LP I/O connector block.

R6868 is 68-pin flat 1-meter long ribbon cable terminated with a 68-pin connector on each end. This cable is used to connect 68-pin E Series DAQ devices, DIO-32HS, or

NI 6533 device to 68-pin accessories. The Figure 2.14 gives the connection of DAQCard 6024E, CB-68LP and ribbon cable R6868 [17].

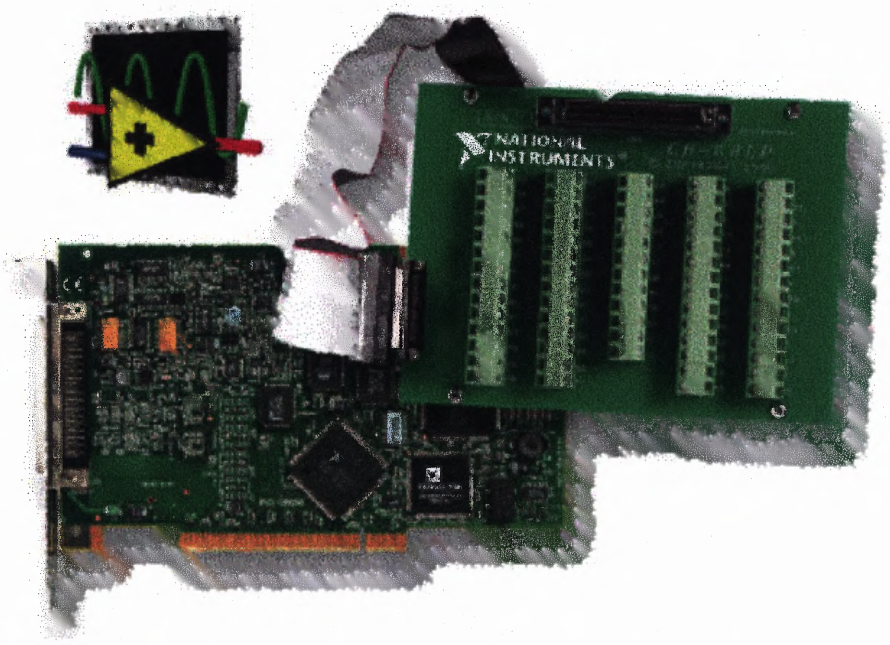


**Figure 2.14** Connection of DAQCard 6024E, CB-68LP and ribbon cable R6868.
Source: National Instruments (NI) Corporation.

## 2.7 Summary

In order for the circuit to switch a current, a voltage source, a ground and a load are required. NI-DAQCard's digital I/O lines have limited current sinking capacity. Therefore, the transistor circuit that was incorporated into the system required the DAQCard to drive the base current of the first transistor to provide higher base current for the second transistor and allow sufficient current to activate the valve.

The solenoid valves provide linear motion when powered. The solenoid armature moves inward when the signal coming into the driver is high. As shown in the transistor circuit, the solenoid is connected between the 5V supply voltage and collector of the second transistor of the darlington pair. This solenoid acts as a load on the driver. When

the input signal of the digital line coming into the solenoid subsystem is high (logic 1), a potential difference across the solenoid causes current to flow. It is this current (>263mA) that causes the solenoid armature to move. In this logic 1 condition, the air from the air compressor to the air muscle can be filled. When the input signal of the digital line coming into the solenoid subsystem is low (logic 0), a potential difference across the solenoid causes current to stop. A spring in the solenoid will cause the armature to move back as soon as the current is turned off. The valves have a 10 msec response time.

# CHAPTER 3

# METHODOLOGY AND RESULTS

## 3.1 Problem Statement

Bang-Bang control and Proportional control methods have been known to exhibit similarities in the human musculoskeletal systems. These systems are very difficult to replicate because the components that comprise them are highly non-linear [20]. Constructing a single degree-of-freedom joint model approached these two situations. The Single DOF joint model is shown in Figure 3.1.

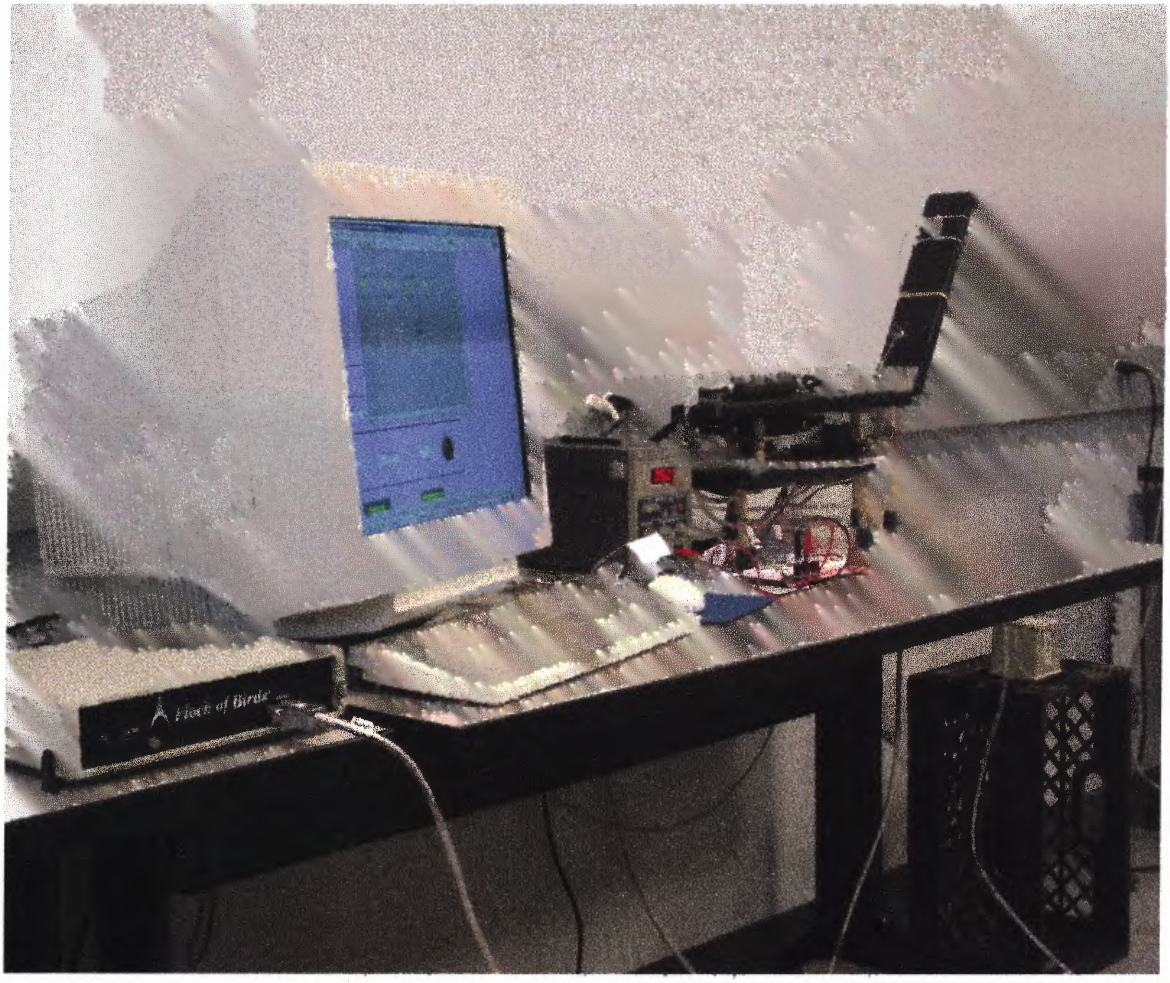


**Figure 3.1** Biologically inspired single joint model.

Single joint enables us to concentrate on fewer joint torques and forces that are abundant in biological systems. Although this approach may not be ideal for modeling such a system, the model was intended to examine force optimization techniques from a control engineering point of view for quick quantitative analysis.

The first approach was the ON/OFF (or Bang-Bang) controller, which is a closed-loop controller. A closed-loop uses a feedback signal to maintain the controlled process at or as close as possible to the desired value. This type of controller is operated by turning the actuator (valve) ON when the desired joint angle is greater than the actual angle value, and OFF when the desired joint angle smaller than the actual angle. The actual angle is measured continuously by Flock of Birds sensor and the desired angle is the user selectable on the LabVIEW program's front panel.

As expected the Bang-Bang control method used in this experiment resulted in instability. Some overshoot occurred due to the limitations of the valves and control of the process variable such as joint angle. This is because the resulting position of the joint exceeded the desired position before the valve could be turned off. Likewise, undershoot occurred because of the end point positions moving higher than the desired position.

A pulse width modulation (PWM) technique is proposed to give digitally timed intervals to improve overall instability [17]. Although the perturbations are expected to be reduced, the system should fail in reaching a critically damped state due to the non-linear nature of the pneumatic muscle.

In addition, a non-linear digital proportional (P) control program is proposed to further alleviate the hysterisis. Now, the system does this by responding to the magnitude of the error (proportional to difference in joint angle). This method should work quite well compare to the above method.

The physical model was constructed of a single joint with an agonist and an antagonist muscle operating under computer control. Utilizing LabVIEW v.6i software, McKibben air muscles and the Flock of Birds sensor, a Bang-Bang closed-loop controller was implemented to exhibit end point position control. The Bang-Bang controller is basically ON/OFF controller. Its output oscillates around the target position. Due to the effect of overshoot and undershoot, the controller was found to be inadequate in maintaining stability in the system. In an effort to alleviate the perturbations, a non-linear digital proportional (P) controller and a program to include pulse width modulated (PWM) output are introduced [16]. The side view of the physical model is shown in the Figure 3.2.

The components used in this model corresponding to the given numbers as shown in the Figure 3.2, are listed in the Table 3.1.

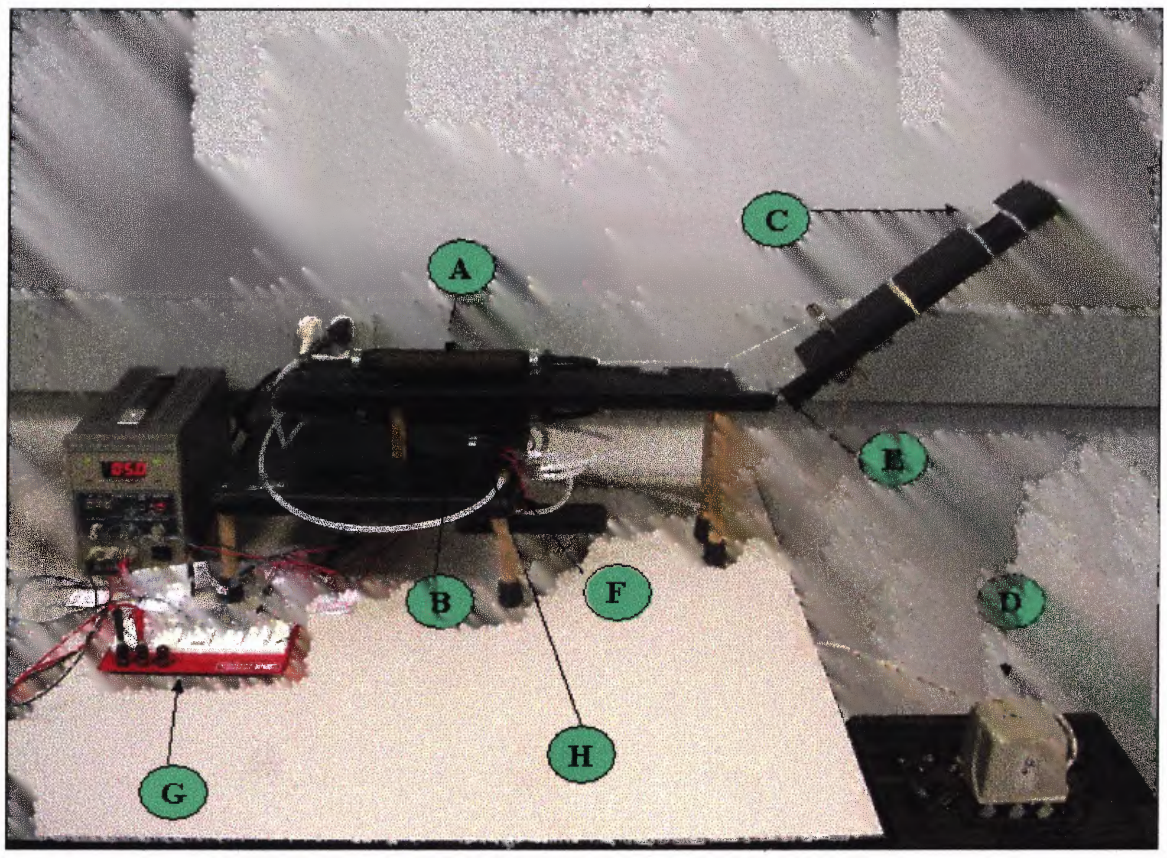


**Figure 3.2** The side view of the physical model.

**Table 3.1** Components used in the Physical Model

| NUMBERS AS IN FIGURE 3.2 | PHYSICAL COMPONENT |
|---|---|
| A | UPPER AIR MUSCLE |
| B | LOWER AIR MUSCLE |
| C | BIRD SENSOR OF FOB UNIT |
| D | TRANSMITTER OF FOB UNIT |
| E | HINGE (FOR MOVEMENT OF ARM) |
| F | ISONIC MANIFOLD |
| G | TRANSISTOR CIRCUIT |
| H | CONTROL VALVES |

### 3.2 Measurement and Automation Explorer

In order for the system to respond appropriately, configurations of the digital I/O channels were required. This was accomplished through the use of NI Measurement and Automation Explorer (MAX) v.2.0 tool that is built into the NI-DAQ driver software [16]. The configuration process allowed us to set the parameters of the digital I/O channels. The configuration setup also allowed testing of the system diagnostics. A panel view of the MAX v.2.0 is shown in the Figure 3.3. The four digital I/O lines were configured for the four solenoid valves. The whole configuration tree can be shown in the panel view of the MAX. There were eight digital I/O lines in the NI-DAQ-Card PCI-6024E. We used four digital I/O lines out of eight. The digital I/O lines 0 and 6 were used for the two solenoid valves, used for the upper muscle activation. The digital I/O lines 2 and 4 were used for the two solenoid valves, used for the lower muscle activation.

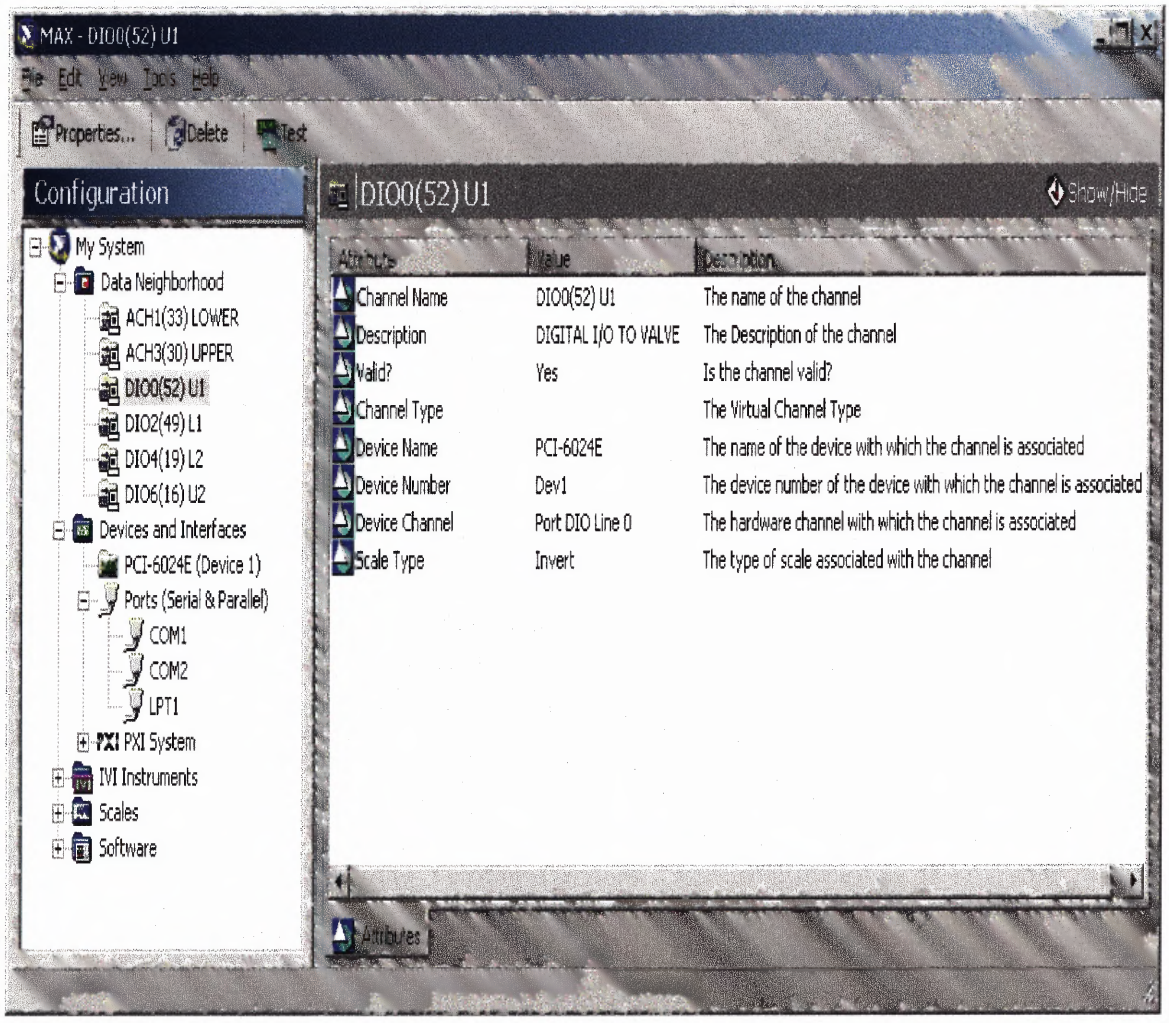


**Figure 3.3** Panel view of the NI-MAX v.2.0.

The corresponding digital I/O of the solenoid valves shown in the Figure 3.4.

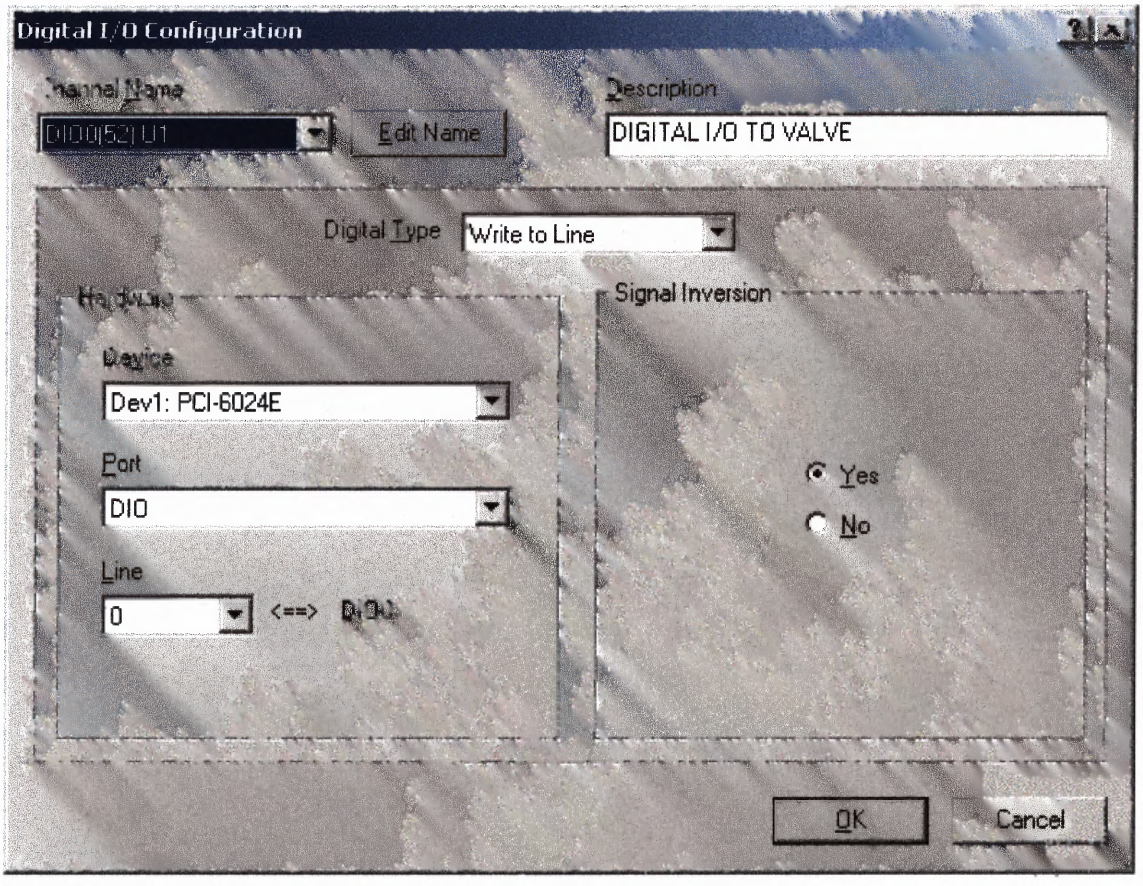


**Figure 3.4** NI MAX digital output configuration.

The initialization of the four solenoid valves using the MAX and LabVIEW software was proposed in the Appendix F. We can control the four solenoid valves using a LabVIEW program shown in Appendix F.

### 3.3 Bang-Bang Control

The Bang-Bang control is basically ON/OFF control. The Bang-Bang method used to control the joint model was accomplished using NI LabVIEW v.6i software (Appendix G). Upon entering an end point position located within 20° - 80° range, at 1 degree increments, the joint moved through the desired location and then back past this point in the opposite direction causing it to oscillate. When the actual angle is less than

the desired target angle, an overshoot occurred. When the actual angle is greater than the desired target angle, an undershoot occurred. The value of the roll angle of the FOB sensor was captured in the program continuously. The Bang-Bang control program demonstrates the hysterisis achieved using this control method, which resulted in perturbations around the desired position. The front panel of the NI LabVIEW Bang-Bang control is shown in Figure 3.5. The Block diagram of VI is shown in the Figure 3.6. The results of the program show that for Bang-Bang control, the system is underdamped. This is an undesirable form of the control for the single joint model. However, the Figure 3.7 shows the graph, which incorporates the Bang-Bang control at 42 degrees.

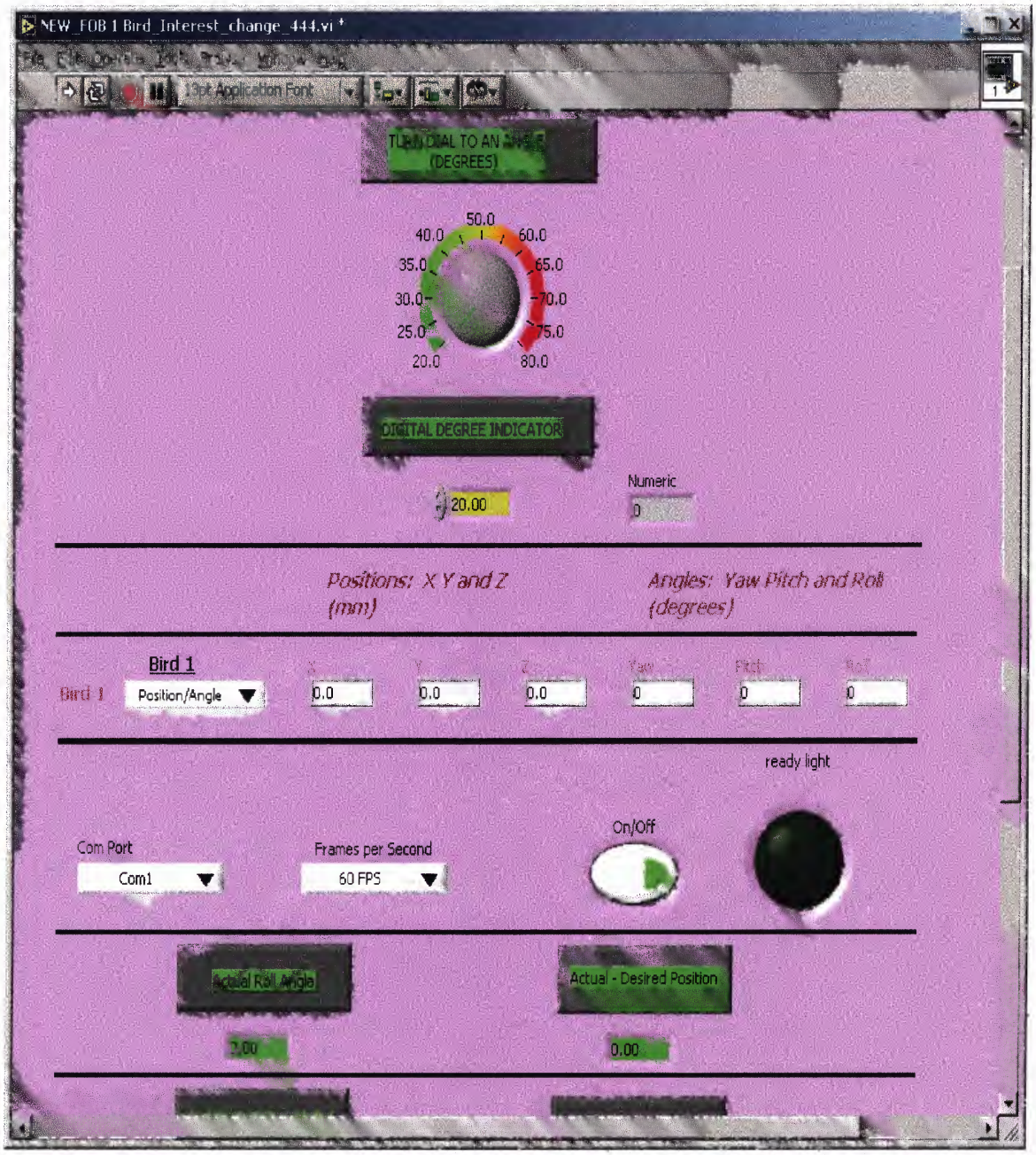


**Figure 3.5** Front panel of NI LabVIEW Bang-Bang control program.

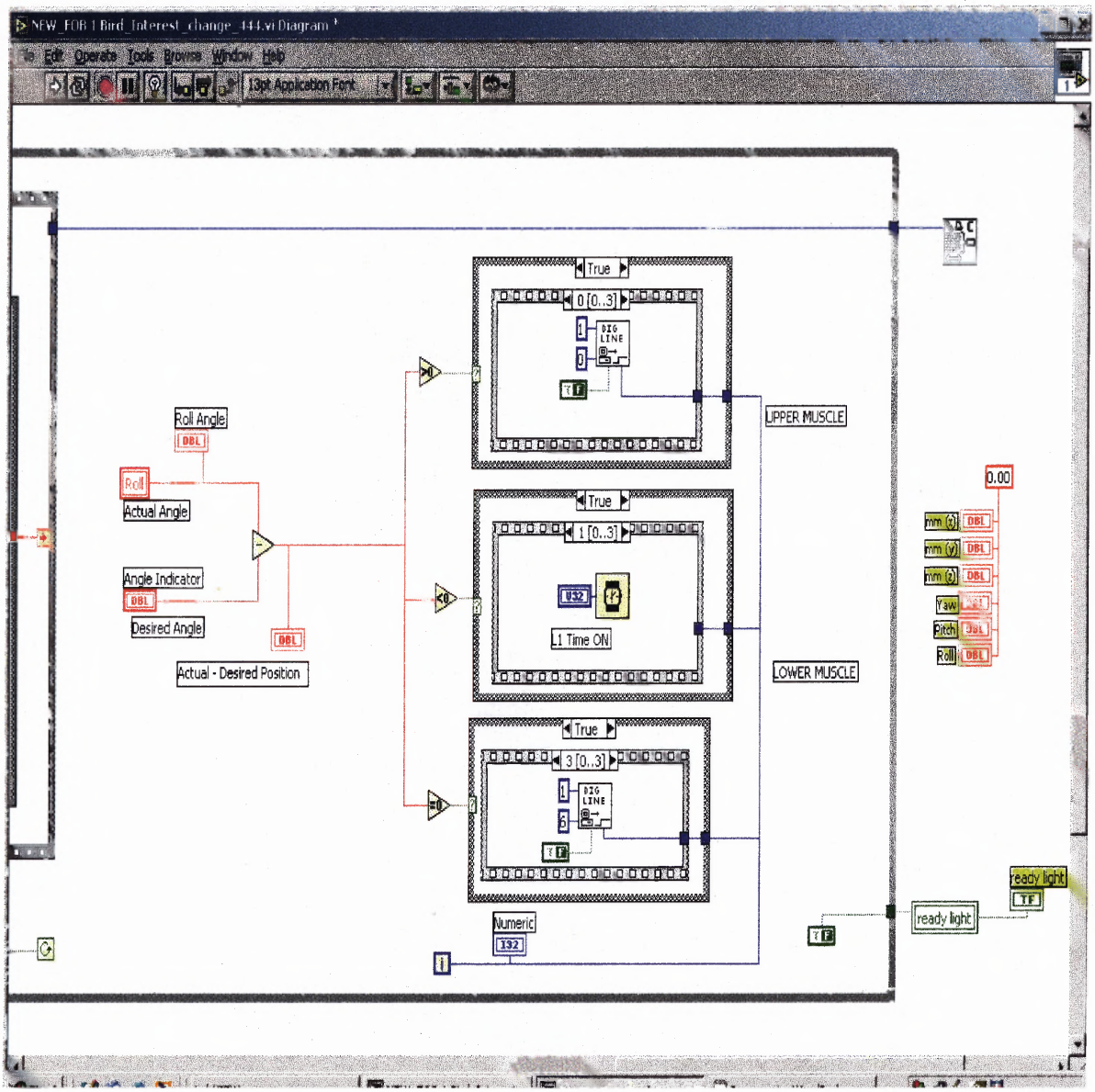


**Figure 3.6** Block diagram of NI LabVIEW Bang-Bang control program.

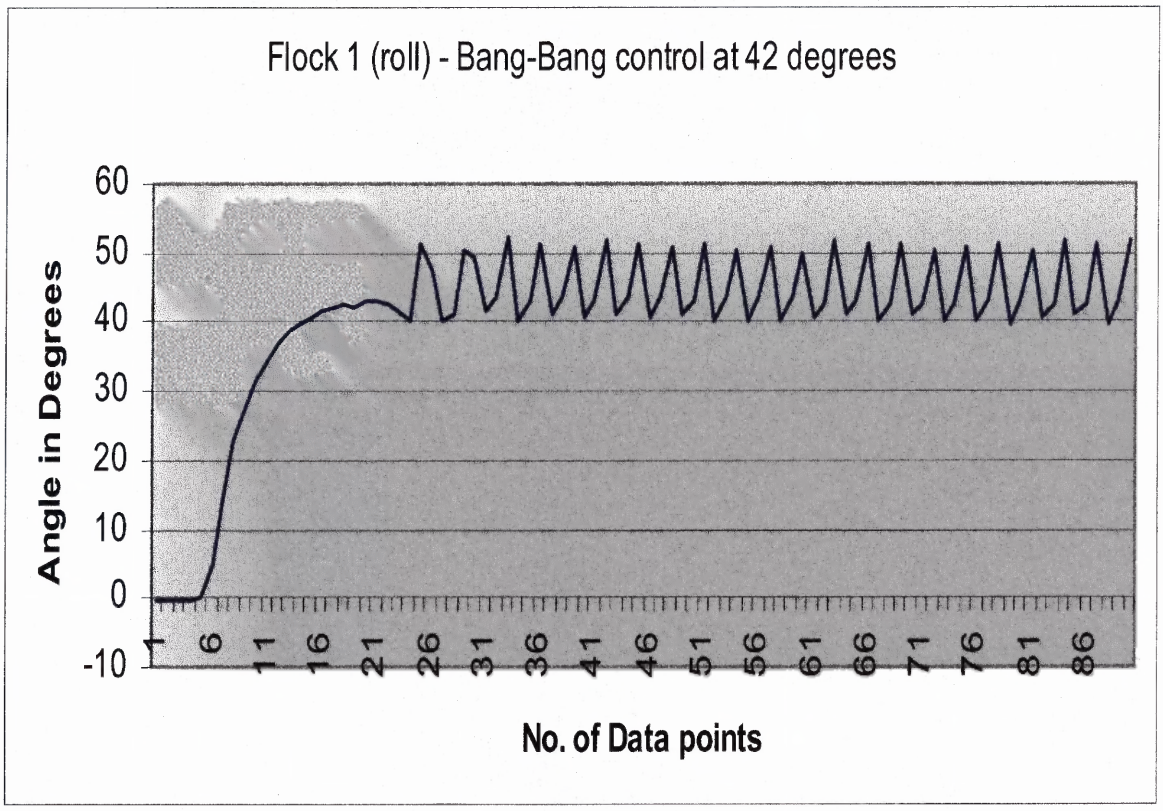


**Figure 3.7** Bang-Bang control output.

The actual angle data oscillates around the target angle. The limitations of the response time of the mead fluid dynamics solenoid valve used decreased the reliability of the system.

### 3.4 Pulse Width Modulation

Pulse Width Modulation (PWM) is a way of digitally encoding the analog signal levels. Through the use of high-resolution counters, the duty-cycle of a square wave is modulated to encode a specific analog signal level. The PWM signal is still digital because, at any given instant of time, the full DC supply is either fully "ON" or fully "OFF" [16]. The voltage or current source is supplied to the analog load by means of a repeating series of on and off pulses. The on-time is the time during which the DC supply is applied to the load, and the off-time is the time period during which that supply

switched off. As long as the response time is sufficient, the solenoid valve can close or open encoded with PWM [12].

The PWM technique is proposed to reduce the power consumption. The goal will be to limit the amount of current supply to the solenoid valves by varying the duty cycle. In doing this, the air muscles will incur a reduction in overshoot and undershoot, reduce overall instability. Although the perturbations are reduced, the system is not expected to reach a critically damped state. A PWM technique has been generated for easy implementation into the VI of the Bang-Bang control method. The simple pulse width modulation LabVIEW program is shown in the Figure 3.8.

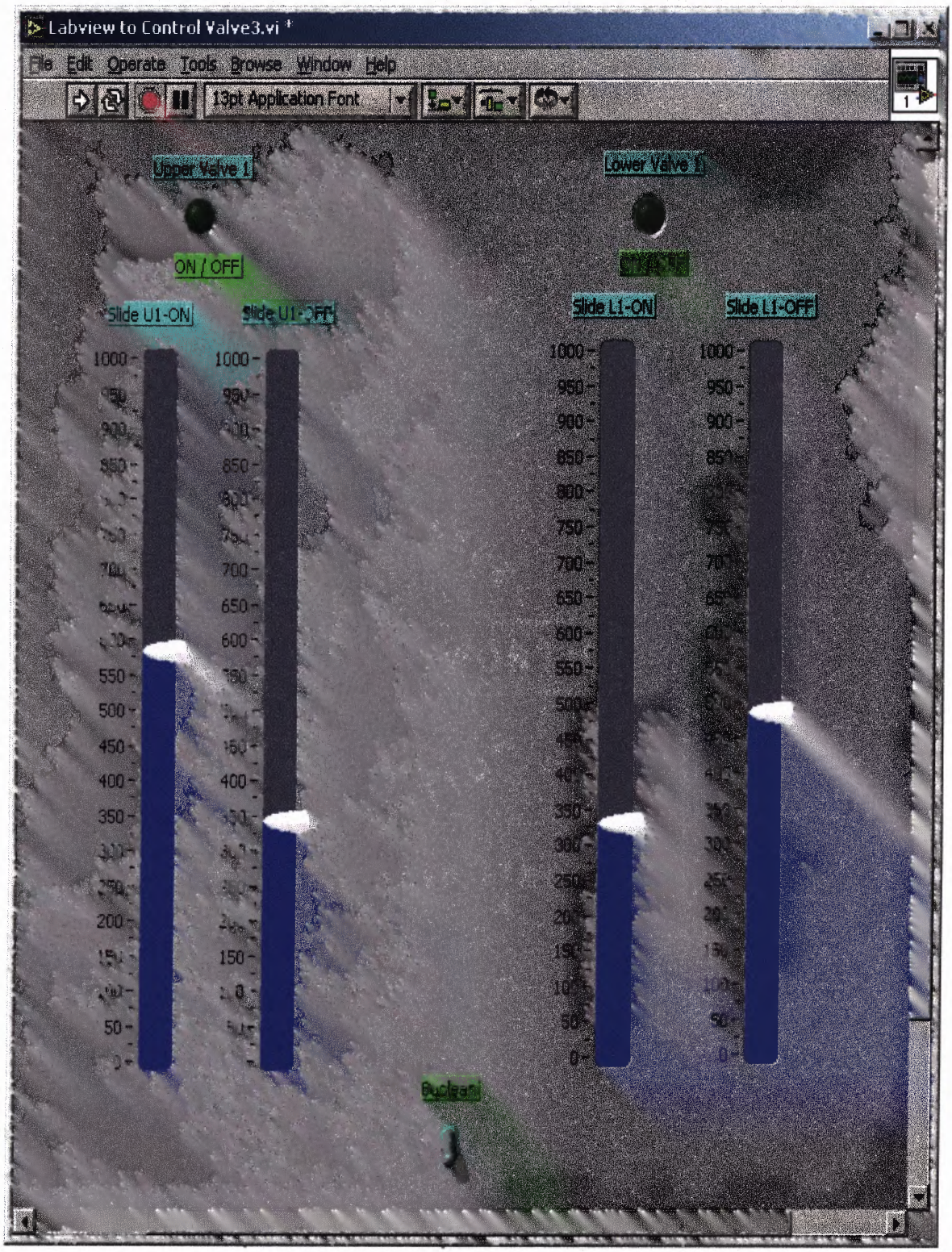


**Figure 3.8** The pulse width modulation LabVIEW program.

### 3.5 Proportional Control

Proportional (P) controllers are pure gain or attenuation controllers. A non-linear digital proportional feedback controller is designed to generate an output that causes some corrective effort to be applied to a process so as to drive a measurable process variable towards a desired value known as the set-point [22]. The controller uses an actuator to affect the process and a FOB sensor to measure the results. For this joint model, a LabVIEW program of a non-linear digital proportional controller is proposed to minimize perturbations (Appendix H).

Most feedback controllers determine their output by observing the error between the current and the desired locations and a measurement of the process variable. A linear proportional controller is identified by the following equation:

P = Proportional Band = 100 / gain

$$u = k_p\, e$$

where, Controller input is error (reference value- output value).

Controller output is a controller signal.

$K_p$ is the proportional gain constant.

P controller involves only a proportional gain (or attenuation).

A non-linear proportional controller is similarly defined by the equation:

$$u = k_p(a)\, e$$

where, the proportional gain is no longer a constant, but is a function of a variable 'a'.

The non-linearity of the pneumatic muscles required that a non-linear gain (duty cycle) be applied to the muscles. Referring to the earlier equation for non-linear proportional controller, the governed expression for the non-linear gain implemented in

this thesis is a function of the angular error, yielding

$$u = k_p(e)\, e$$

Proportional controller increases the gain, which upgrade both steady-state and transient responses. As a result the steady-state error reduces. The non-linear digital proportional control output will control the digital output channels to the solenoid valves. Theoretically the LabVIEW program should reduce the fluctuations in the system but accurate tuning of the digital proportional mode is essential. One important thing is that, the activation of an air muscle does not require the current, but uses the air volume to vary muscle force. The digital proportional program will eventually replace the Bang-Bang method of control. The end result will be to generate a controller output that steadily drives the process variable in the direction required to eliminate the error [22].

The Table 3.2 and Table 3.3 show the chart of the relationship between the degrees and the operating time of the valves for agonist and antagonist muscle. If the difference between the desired angle and actual angle is positive, the error is considered as positive error. If the difference between the desired angle and actual angle is negative, the error is considered as negative error. It describes the corresponding error of degree interval (desired angle - actual angle) to the time of operation of the valves to the upper and lower muscle.

**Table 3.2** Degree v.s. Time of the Upper Muscle for Positive Degree Error

| CASE | ANGLE (Desired - Actual) (Degree) | UPPER MUSCLE ON TIME (msec) | UPPER MUSCLE OFF/HOLD TIME (msec) | DUTY CYCLE (%) |
|---|---|---|---|---|
| 1 | >=20 | 50 | 0 | 100 |
| 2 | >=15 & <20 | 45 | 10 | 81.82 |
| 3 | >=8 & <15 | 40 | 10 | 80 |
| 4 | >=7 & <8 | 35 | 15 | 70 |
| 5 | >=6 & <7 | 30 | 20 | 60 |
| 6 | >=5 & <6 | 25 | 25 | 50 |
| 7 | >=4 & <5 | 20 | 30 | 40 |
| 8 | >=3 & <4 | 15 | 35 | 30 |
| 9 | >=2 & <3 | 10 | 10 | 50 |
| 10 | >=1 & <2 | 5 | 10 | 33.33 |
| 11 | >=0 & <1 | 0 | 0 | 0 |

**Table 3.3** Degree v.s. Time of the Lower Muscle for Negative Degree Error

| CASE | ANGLE (Desired-Actual) (Degree) | LOWER MUSCLE ON TIME (msec) | LOWER MUSCLE OFF/HOLD TIME (msec) | DUTY CYCLE (%) |
|---|---|---|---|---|
| 1 | <=(-20) | 50 | 0 | 100 |
| 2 | <=(-15) & >(-20) | 45 | 10 | 81.82 |
| 3 | <=(-8) & >(-15) | 40 | 10 | 80 |
| 4 | <=(-7) & >(-8) | 35 | 15 | 70 |
| 5 | <=(-6) & >(-7) | 30 | 20 | 60 |
| 6 | <=(-5) & >(-6) | 25 | 25 | 50 |
| 7 | <=(-4) & >(-5) | 20 | 30 | 40 |
| 8 | <=(-3) & >(-4) | 15 | 35 | 30 |
| 9 | <=(-2) & >(-3) | 0 | 0 | 0 |
| 10 | <=(-1) & >(-2) | 0 | 0 | 0 |
| 11 | <=0 & >(-1) | 0 | 0 | 0 |

The pulse width modulation relies upon a fast duty cycle of the valves and makes the different cases for the system. The Figure 3.9 shows the graph to get 40 degrees by implementing the proportional control. The Figure 3.10 shows the graph to get the sequence of the desired angle values (35° - 20° - 40°). The Figure 3.11 shows the transitions of the desired angle values (35° - 30° - 25° - 20°).

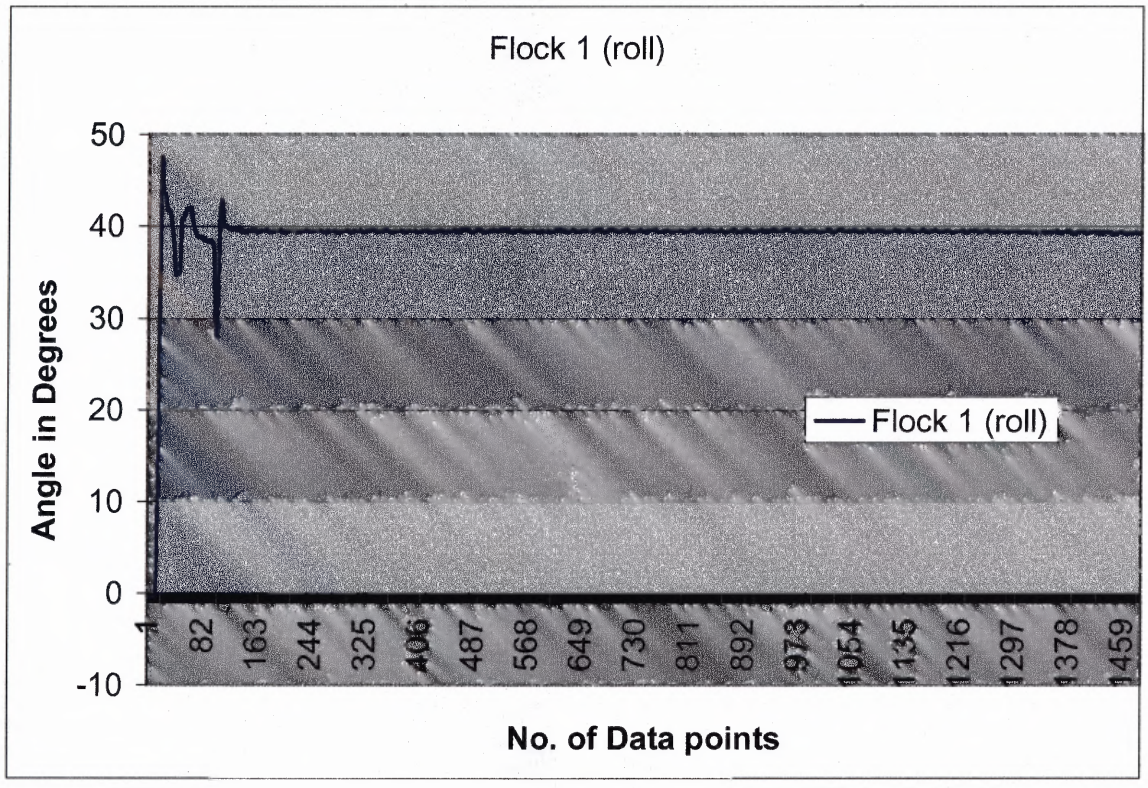


**Figure 3.9** Non-linear proportional control at 40 degrees value.

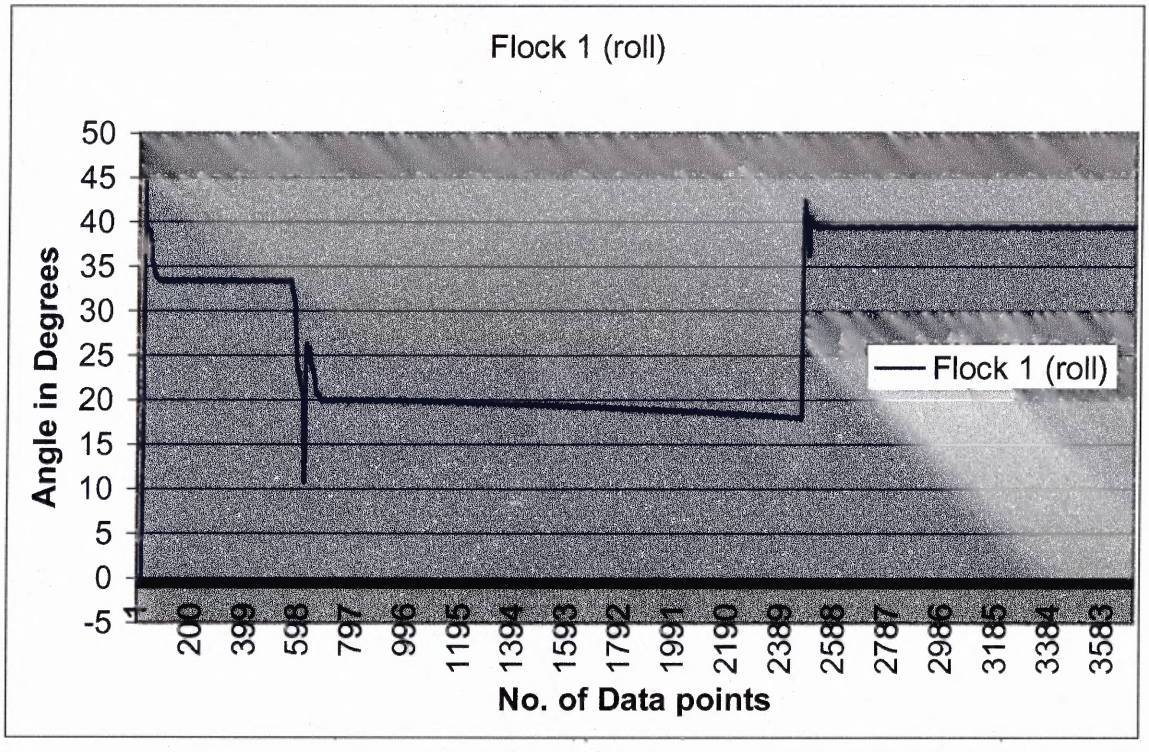


**Figure 3.10** Non-linear proportional control at 35° - 20° - 40° values.

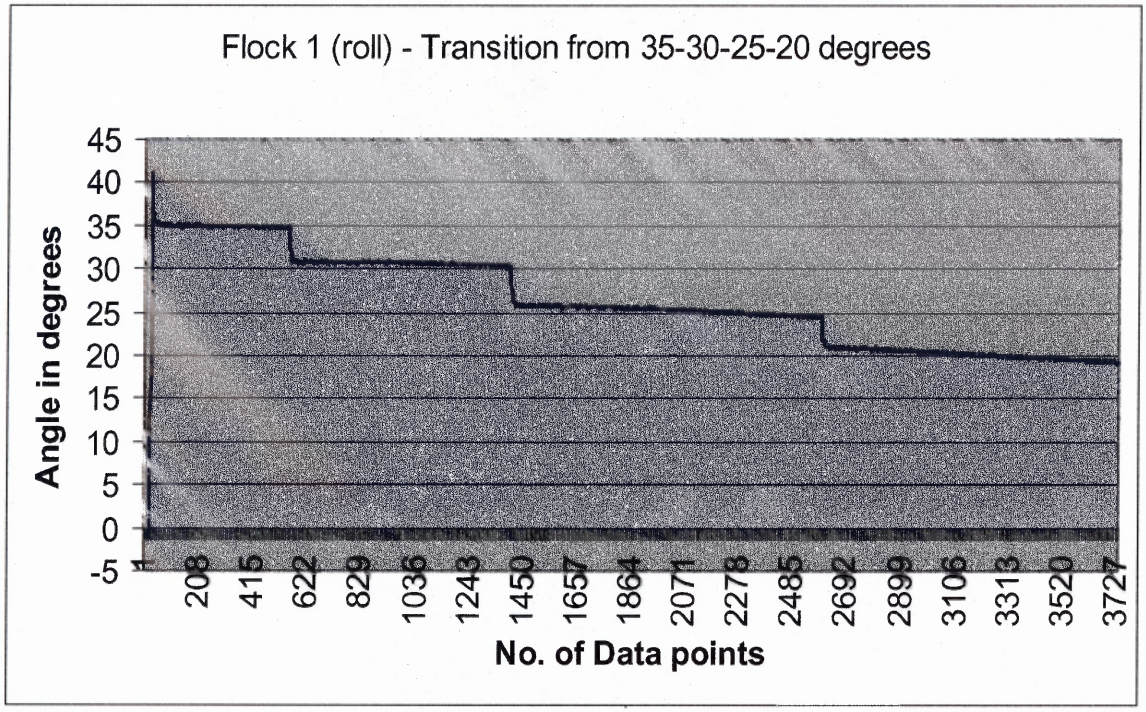


**Figure 3.11** Non-linear proportional control at 35°-30°-25°-20° values.

### 3.6 Summary

Initially the Bang-Bang (an ON/OFF) closed loop controller was introduced. Some perturbations occurred due to the limitations of the valves and the control of the process variable. The overshoot occurred because of the end point positions moving lower than the desired position. Likewise, undershoot occurred because of the end point positions moving higher than the desired position. This resulted in a feedback value incapable of maintaining the controlled process at the desired position value.

Further the concept of PWM was introduced to alter the digital output signal in an attempt to better control the system. With the use of PWM, the reduction of air coming into the air muscles greatly enhances the stability. Furthermore, the implementation of a non-linear digital proportional controller is suggested as a more appropriate means of controlling the single DOF (degree of freedom) joint.

# CHAPTER 4

# CONCLUSION

In the biologically inspired joint model, the author initially demonstrated control by the Bang-Bang method. Results show that this method of control for achieving single plane movements is not optimum due to the resulting perturbations. In an effort to reduce the hysterisis, a LabVIEW program implementing a pulse width modulated, non-linear digital proportional controller is proposed. Reproducing non-linear biological systems for quantitative analysis encompasses detailed knowledge of the control mechanisms in biological systems as well as an understanding of control engineering methodology.

Controlling movement of a joint requires co-activation of agonist and antagonist muscles. Essentially, a force needs to be applied to one muscle to get the joint moving, and activation of the other muscle to act as a brake. This in turn, slows the joint, letting it achieve the desired target angle.

The Bang-Bang (ON/OFF) control method has perturbations about the desired target angle. Limitations of the Bang-Bang control method brought the investigation into other possible methods of control. The concept of pulse width modulation is introduced as a powerful technique for controlling the digital outputs. The LabVIEW program runs and asks for the destination file name to user for store the roll angle data continuously at 60 frames per second. The plot of Bang-Bang controller is shown in Figure 3.7. The graph shows the perturbations present about the desired target angle. The perturbations are about 10 degrees of range.

Furthermore, a non-linear digital proportional control method is introduced as future means of increasing stability. The plot of proportional controller is shown in the

Figure 3.9. The graph shows that the desired angle is achieved through the non-linear pattern. Implemented a novel controller that is appropriate for non-linear pneumatic muscles, which allows for accurate and stable movement of a single DOF joint.

## APPENDIX A

## FOB TECHNICAL & PHYSICAL SPECIFICATIONS

This appendix describes the technical and physical specifications of Flock of Birds sensor used in the system.

**Physical Specifications:**

| | |
|---|---|
| Transmitter: | 3.75" (9.6cm) cube (mounted inside enclosure or external) with 10' (3.05m) cable |
| Sensor: | 1.0" x 1.0" x0.8" cube (or optional 3-button mouse) with 10' or optional 35' cable |
| Enclosure: | 9.5" x 11.5" x 2.6" (24cm x 29cm x 6.6cm) |

**Technical Specifications:**

| | |
|---|---|
| Tracking range: | ± 4'(1.2m) ±10'(3.05m) optional in any direction |
| Angular range: | ±180° Azimuth & Roll, ±90° Elevation |
| Static Accuracy: | Position: 0.07" (1.8mm) RMS<br>Orientation: 0.5° RMS |
| Static Resolution: | Position: 0.02' (0.5mm) @ 12" (30.5cm)<br>Orientation: 0.1° @ 12" (30.5cm) |
| Update Rate: | Up to 144 measurements/second |
| Outputs: | X, Y, Z positional coordinates and orientation angles, or rotation matrix |
| Interface: | RS-232 with selectable baud rates to 115,200 |
| Format: | Binary |
| Modes: | Point to Stream (RS232 only) |

**Electrical Specification:**

| | |
|---|---|
| Power: | +5V DC @ 2.45 amps avg., 3.85 amps peak<br>+12V DC @ 0.53 amps avg., 0.63 amps peak |

| | |
|---|---|
| Environment: | All specifications are valid at 30° C ± 10° in an environment void of large metal objects and electromagnetic frequencies, other than the power line. |
| Operating Humidity: | 10% to 90% non-condensing |

Source: Ascension Technology Corporation.

## APPENDIX B

## DIPSWITCH SETTINGS FOR NORMAL ADDRESS MODE

This appendix describes the selection of dipswitch settings, which are located on back panel of electronic controller unit. For this program author selected 115200 as the Baud Rate.

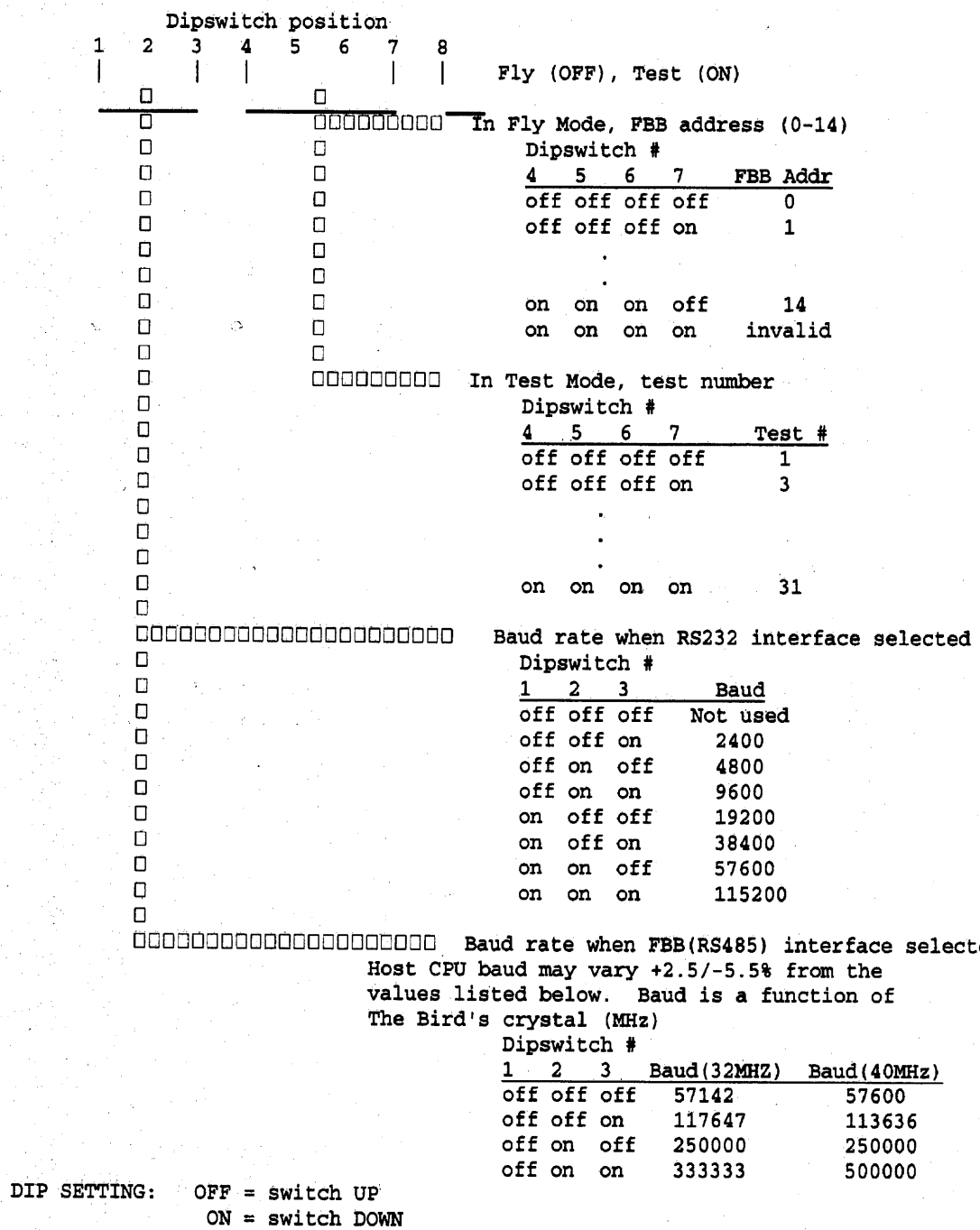


DIP SETTING: OFF = switch UP
ON = switch DOWN

# APPENDIX C

## SPECIFICATION OF MEAD FLUID DYNAMICS VALVE

This appendix describes the specification of mead fluid dynamics valve. Mead Fluid Dynamics Inc manufactures the valves used in this model. The Isonic solenoid valves contain an integrated electronics board with surge suppression and an LED. Mead's patented "half-shell" design of the three-way valves allows flow channels and component compartments to be designed directly into the body. The technical specifications of the control valve are shown in the next page.

# Isonic® (2 and 3-Way)

| Specifications | |
|---|---|
| Design: | Poppet |
| Media: | Air or Inert Gas |
| Lubrication: | None Required |
| Filtration: | 40 micron |
| Cycle Life: | 50,000,000 cycles |
| Orifice Size: | A: 0.025"/0.65mm |
| | B: 0.035"/0.90mm |
| | C: 0.055"/1.4mm |
| Flow: | A: 0.01$C_v$ |
| | B: 0.02$C_v$ |
| | C: 0.05$C_v$ |
| Maximum Pressure: | A: 120 PSI/8.3 Bar |
| | B: 120 PSI/8.3 Bar |
| | C: 30 PSI/2.1 Bar |
| Vacuum: | to 28 in. Hg |
| Temperature Range: | 0° - 120°F/49°C |
| Tubing: | ⅛" or 4mm |
| Mounting Holes: | 0.156 diameter (1 hole, 1 slot) |
| Seals: | Viton® and Nitrile |
| Weight: | 1.5 oz. (per valve) |

## Solenoid Data

| Voltage | 5DC | 12DC | 24DC | 24AC | 120 AC | 230AC |
|---|---|---|---|---|---|---|
| Amps | 0.320 | 0.133 | 0.058 | 0.058 | 0.014 | 0.014 |
| Resistance | 15Ω | 92Ω | 400Ω | 400Ω | 8550Ω | 30,000Ω |
| Initial Power | 1.6 | 1.6 | 1.4 | 1.4 | 1.7 | 3.4 |
| Continuous Os | 1.3 | 1.3 | 1.2 | 1.2 | 1.5 | 3.0 |

**Response Time:** 10 milliseconds

**Molex Connector:** UL and CSA Listed

**Din Connector:** Protection Class- IP 65 according to DIN 40 050
Insulation Class- Group C according to VDE 0110
Conform to DIN 43650 Form C Specifications

## Manifold

**Common Air Inlet:** Built-in, push-in fittings for ¼" OD or 6mm tubing both ends

**Foot Mounting:** 4 slots, 11/64" diameter

**DIN Rail Mounting:** Attaches to 15mm DIN rail

## Dimensions

**Valves:**

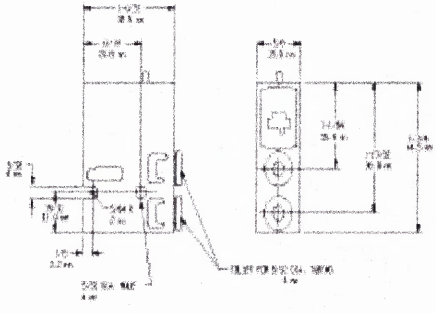

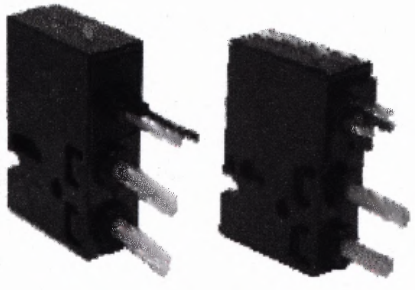

**Manifolds**

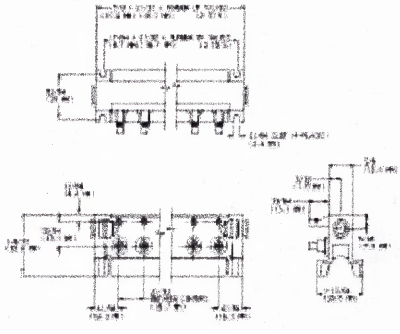

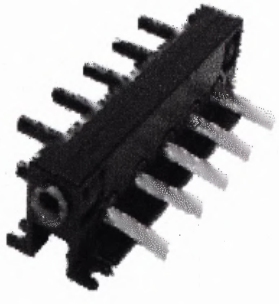

# APPENDIX D

## SPECIFICATIONS OF NI-DAQCARD-AI-16E-4

This appendix describes the technical specifications of NI-DAQCard-AI-16E-4 used in the system.

# E Series Multifunction DAQ Specifications

## 12-Bit E Series (NI 607xE, NI 606xE, NI 604xE, NI 602xE)

These specifications are typical for 25 °C unless otherwise noted.

### Analog Input

Accuracy specifications ..... See tables in E Series Product pages.

#### Input Characteristics

Number of channels

| | |
|---|---|
| 6070E<br>6060E<br>6062E<br>604xE<br>602xE | 16 single-ended or 8 differential<br>(software selectable per channel) |
| 6071E<br>6061E | 64 single-ended or 32 differential<br>(software selectable per channel) |

Type of ADC ..... Successive approximation
Resolution ..... 12 bits, 1 in 4,096
Maximum sampling rate

| | |
|---|---|
| 607xE | 1.25 MS/s |
| 606xE | 500 kS/s |
| 604xE | 500 kS/s single-channel scanning<br>250 kS/s multichannel scanning |
| 6061E | 500 kS/s single-channel scanning<br>333 kS/s multichannel |
| 6023E<br>6024E<br>6025E | 200 kS/s |
| 6020E<br>6021E | 100 kS/s |

Streaming-to-disk rate (system dependent)[1]

| | |
|---|---|
| 607xE | 1.25 MS/s |
| 606xE | 500 kS/s |
| 604xE | 250 kS/s |
| 6023E<br>6024E<br>6025E | 200 kS/s |
| 6020E<br>6021E | 100 kS/s[2] |

[1]Streaming-to-disk rates do not apply to RT Series devices.
[2]DAQPad™-6020E rates with SCSI or DMA-enabled EIDE.

Input signal ranges

| Device | Range (Software Selectable) | Input Range | |
|---|---|---|---|
| | | Bipolar | Unipolar |
| 607xE | 20 V | ±10 V | – |
| 606xE | 10 V | ±5 V | 0 to 10 V |
| 604xE | 5 V | ±2.5 V | 0 to 5 V |
| 6020E | 2 V | ±1 V | 0 to 2 V |
| 6021E | 1 V | ±500 mV | 0 to 1 V |
| | 500 mV | ±250 mV | 0 to 500 mV |
| | 200 mV | ±100 mV | 0 to 200 mV |
| | 100 mV | ±50 mV | 0 to 100 mV |
| 6023E | 20 V | ±10 V | – |
| 6024E | 10 V | ±5 V | – |
| 6025E | 1 V | ±500 mV | – |
| | 100 mV | ±50 mV | – |

Input coupling ..... DC
Maximum working voltage
(signal + common mode) ..... Input should remain within ±11 V of ground

Overvoltage protection

| Device | Powered On | Powered Off |
|---|---|---|
| 607xE<br>606xE<br>604xE | ±25 V | ±15 V |
| 6023E<br>6024E<br>6025E | ±40 V | ±25 V |
| 6020E<br>6021E | ±35 V | ±25 V |

Inputs protected

| | |
|---|---|
| 6070E, 6060E<br>6062E, 604xE<br>602xE | ACH<0..15>, AISENSE |
| 6071E, 6061E | ACH<0..63>, AISENSE, AISENSE2 |

FIFO buffer size

| | |
|---|---|
| AT-MIO-16E-1<br>DAQCard-6062E | 8,192 samples |
| DAQPad-6020E | 4,096 samples |
| 6060E/6061E<br>DAQPad-6070E<br>DAQCard-6024E | 2,048 samples |
| 6041E | 1,024 samples |
| PCI-MIO-16E-1<br>PXI-6070E<br>6071E, 6040E<br>PCI-602xE<br>(except DAQPad)<br>PXI-6025E | 512 samples |

Data transfers
PCI, PXI, AT, DAQPad for IEEE 1394..... DMA, interrupts, programmed I/O
DAQCard, DAQPad for USB ..... Interrupts, programmed I/O
DMA modes
PCI, PXI, DAQPad for IEEE 1394..... Scatter-gather (single-transfer, demand transfer)
AT ..... Single transfer, demand transfer
Configuration memory size ..... 512 words

#### Transfer Characteristics

Relative accuracy

| Device | Typical Dithered | Maximum Undithered |
|---|---|---|
| 607xE<br>606xE<br>604xE<br>6023E<br>6024E<br>6025E | ±0.5 LSB | ±1.5 LSB |
| 6020E<br>6021E | ±0.2 LSB | ±1.5 LSB |

DNL

| Device | Typical | Maximum |
|---|---|---|
| 607xE<br>6060E<br>6061E<br>604xE<br>6023E<br>PCI-6024E<br>6025E | ±0.5 LSB | ±1.0 LSB |
| 6020E<br>6021E | ±0.2 LSB | ±1.0 LSB |
| 6062E<br>DAQCard-6024E | ±0.75 LSB | -0.9, +1.5 LSB |

No missing codes ..... 12 bits, guaranteed

## 12-Bit E Series (NI 607xE, NI 606xE, NI 604xE, NI 602xE) (continued)

### Amplifier Characteristics

Input impedance

| Device | Normal Powered On | Powered Off | Overload |
|---|---|---|---|
| 6070E<br>606xE<br>6040E<br>PCI-6071E<br>PXI-6071E | 100 GΩ in parallel with 100 pF | 820 Ω | 820 Ω |
| 6041E | 100 GΩ in parallel with 100 pF | 1 kΩ | 1 kΩ |
| 602xE | 100 GΩ in parallel with 100 pF | 4.7 kΩ | 4.7 kΩ |

Input bias current ..... ±200 pA
Input offset current ..... ±100 pA

CMRR, DC to 60 Hz

| Device | Range | CMRR |
|---|---|---|
| 607xE | 20 V | 95 dB |
| 6060E | 10 V | 100 dB |
| 6061E | 100 mV to 5 V | 106 dB |
| 604xE | 10 to 20 V | 85 dB |
| 6062E | 5 V | 95 dB |
| | 100 mV to 2 V | 100 dB |
| 6023E | 10 to 20 V | 85 dB |
| 6024E | 100 mV to 1 V | 90 dB |
| 6025E | | |
| 6020E | 100 mV to 20 V | 90 dB |
| 6021E | | |

### Dynamic Characteristics

Bandwidth

| Device | Small Signal (-3 dB) | Large Signal (1% THD) |
|---|---|---|
| 607xE | 1.6 MHz | 1 MHz |
| 6060E/6061E | 1 MHz | 300 kHz |
| 6062E | 1.3 MHz | 250 kHz |
| 6041E | 800 kHz | 400 kHz |
| 6040E | 600 kHz | 350 kHz |
| 6023E<br>PCI-6024E<br>6025E | 500 kHz | 225 kHz |
| DAQCard-6024E | 500 kHz | 265 kHz |
| 6021E | 150 kHz | 120 kHz |

Settling time to full-scale step

| Device | Range | Accuracy ±0.012% (±0.5 LSB) | Accuracy ±0.024% (±1 LSB) | Accuracy ±0.098% (±4 LSB) |
|---|---|---|---|---|
| 6070E | 20 V | 2 µs typical<br>3 µs max | 1.5 µs typical<br>2 µs max | 1.5 µs typical<br>2 µs max |
| | 10 V | 2 µs typical<br>3 µs max | 1.5 µs typical<br>2 µs max | 1.3 µs typical<br>1.5 µs max |
| | 200 mV to 5 V | 2 µs typical<br>3 µs max | 1.5 µs typical<br>2 µs max | 0.9 µs typical<br>1 µs max |
| | 100 mV | 2 µs typical<br>3 µs max | 1.5 µs typical<br>2 µs max | 1 µs typical<br>1.5 µs max |
| PCI-6071E<br>PXI-6071E | 20 V | 3 µs typical<br>5 µs max | 1.9 µs typical<br>2.5 µs max | 1.9 µs typical<br>2 µs max |
| | 10 V | 3 µs typical<br>5 µs max | 1.9 µs typical<br>2.5 µs max | 1.2 µs typical<br>1.5 µs max |
| | 200 mV to 5 V | 3 µs typical<br>5 µs max | 1.9 µs typical<br>2.5 µs max | 1.2 µs typical<br>1.3 µs max |
| | 100 mV | 3 µs typical<br>5 µs max | 1.9 µs typical<br>2.5 µs max | 1.2 µs typical<br>1.5 µs max |
| 6060E | All | 2 µs typical<br>4 µs max | 1.9 µs typical<br>2 µs max | 1.8 µs typical<br>2 µs max |
| 6061E | | 5 µs max | 3 µs max | 2 µs max |
| 6062E | All | 2.5 µs typical<br>4 µs max | 2.5 µs typical<br>3 µs max | 2 µs typical<br>2.5 µs max |
| 604xE | All | 4 µs typical<br>8 µs max | 4 µs max | 4 µs max |
| 6023E<br>6024E<br>6025E | All | 5 µs typical | 5 µs max | 5 µs max |
| 6020E<br>6021E | All | 10 µs max | 10 µs max | 10 µs max |

System noise (LSBrms, not including quantization)

| Device | Range | Dither Off | Dither On |
|---|---|---|---|
| 6070E | 1 to 20 V | 0.25 | 0.5 |
| PCI-6071E | 500 mV | 0.4 | 0.6 |
| PXI-6071E | 200 mV | 0.5 | 0.7 |
| | 100 mV | 0.8 | 0.9 |
| 6060E | 200 mV | 0.3 | 0.6 |
| 6061E | 100 mV | 0.5 | 0.7 |
| 6062E | 1 to 20 V | 0.25 | 0.6 |
| | 500 mV | 0.4 | 0.75 |
| | 200 mV | 0.5 | 0.8 |
| | 100 mV | 0.8 | 1.0 |
| 604xE | 1 to 20 V | 0.2 | 0.5 |
| | 500 mV | 0.25 | 0.5 |
| | 200 mV | 0.5 | 0.7 |
| | 100 mV | 0.9 | 1.0 |
| 6023E | 1 to 20 V | 0.1 | 0.6 |
| PCI-6024E, 6025E | 100 mV | 0.7 | 0.8 |
| DAQCard-6024E | 10 to 20 V | 0.1 | 0.65 |
| | 1 V | 0.45 | 0.65 |
| | 100 mV | 0.70 | 0.90 |
| 6020E | 1 to 20 V | 0.07 | 0.5 |
| 6021E | 500 mV | 0.12 | 0.5 |
| | 200 mV | 0.25 | 0.6 |
| | 100 mV | 0.5 | 0.7 |

Crosstalk, DC to 100 KHz

| Device | Adjacent Channels | All Other Channels |
|---|---|---|
| 607xE, 606xE, 604xE | -75 dB | -90 dB |
| 602xE | -60 dB | -80 dB |

# E Series Multifunction DAQ Specifications

## 12-Bit E Series (NI 607xE, NI 606xE, NI 604xE, NI 602xE) (continued)

### Analog Output

#### Output Characteristics

Number of channels

| | |
|---|---|
| 607xE<br>606xE<br>6040E<br>6020E<br>6021E<br>6024E<br>6025E | 2 voltage outputs |
| 6041E<br>6023E | None |

Resolution ..... 12 bits, 1 in 4096
Type of DAC ..... Double buffered, multiplying
Maximum update rate

| Device | Waveform Generation | | | |
|---|---|---|---|---|
| | FIFO Mode | | Non-FIFO Mode | |
| | Internally Timed | Externally Timed | 1 Channel | 2 Channels |
| 607xE<br>6060E, 6061E<br>6040E | 1 MS/s | 950 kS/s | 800 kS/s, system dependent | 400 kS/s, system dependent |
| 6062E | 850 kS/s | 850 kS/s | 800 kS/s, system dependent | 400 kS/s, system dependent |
| 6023E<br><br>PCI-6024E<br>6025E | N/A | N/A | 10 kS/s with DMA<br>1 kS/s with interrupts<br>system dependent | 10 kS/s with DMA<br>1 kS/s with interrupts<br>system dependent |
| DAQCard-6024E | N/A | N/A | 1 kS/s with interrupts<br>system dependent | 1 kS/s with interrupts<br>system dependent |
| 6020E; except DAQPad-6020E | N/A | N/A | 100 kS/s, system dependent | 100 kS/s, system dependent |
| DAQPad-6020E | N/A | N/A | 20 S/s, system dependent | 20 S/s, system dependent |

FIFO buffer size

| | |
|---|---|
| 607xE, 606xE | 2,048 samples |
| 6040E | 512 samples |
| 602xE | None |

Data transfers
- PCI, PXI, AT, DAQPad for IEEE 1394 ..... DMA, interrupts, programmed I/O
- DAQCard, DAQPad for USB ..... Interrupts, programmed I/O

DMA modes
- PCI, PXI, DAQPad ..... Scatter-gather (single transfer, demand transfer)
- AT ..... Single transfer, demand transfer

#### Transfer Characteristics

Relative accuracy
- After calibration (6062E, DAQCard-6024E) ..... ±0.5 LSB typical, ±1.0 LSB max
- After calibration (all others) ..... ±0.3 LSB typical, ±0.5 LSB max
- Before calibration ..... ±4 LSB max

DNL
- After calibration (6062E, DAQCard-6024E) ..... ±0.5 LSB typical, ±1.0 LSB max
- After calibration (all others) ..... ±0.3 LSB typical, ±1.0 LSB max
- Before calibration ..... ±3 LSB max

Monotonicity ..... 12 bits, guaranteed after calibration
Gain error (relative to external reference)
- 6062E ..... ±0.5% of output max, not adjustable
- All others ..... 0 to 0.67% of output max, not adjustable

#### Voltage Output

Ranges

| | |
|---|---|
| 607xE, 6060E<br>6061E, 6040E<br>6020E, 6021E | ±10 V, 0 to 10 V, ±EXTREF, 0 to EXTREF; software selectable |
| 6062E | ±10 V, ±EXTREF, software selectable |
| 6020E, 6021E<br>6024E, 6025E | ±10 V |

Output coupling ..... DC
Output impedance ..... 0.1 Ω max
Current drive ..... ±5 mA max
Protection ..... Short-circuit to ground
Power-on state ..... 0 V (±200 mV)

External reference input (not available on 6024E or 6025E)
- Range ..... ±11 V
- Overvoltage protection

| | |
|---|---|
| 607xE<br>606xE<br>604xE | ±25 V powered on, ±15 V powered off |
| 602xE | ±35 V powered on, ±25 V powered off |

- Input impedance ..... 10 kΩ
- Bandwidth (-3 dB)

| | |
|---|---|
| 607xE<br>6060E, 6061E<br>604xE | 1 MHz |
| 6062E | 50 kHz |
| 602xE | 300 kHz |

#### Dynamic Characteristics

Settling time and slew rate

| Device | Settling Time for Full-Scale Step | Slew Rate |
|---|---|---|
| 607xE<br>606xE<br>6040E | 3 µs to ±0.5 LSB accuracy | 20 V/µs |
| 602xE | 10 µs to ±0.5 LSB accuracy | 10 V/µs |

Noise ..... 200 µVrms, DC to 1 MHz
Glitch energy (at mid-scale transition)
- Magnitude

| Device | Reglitching Disabled | Reglitching Enabled |
|---|---|---|
| DAQPad-6070E<br>PCI-MIO-16E-1<br>PCI-6071E<br>PXI-6070E<br>PXI-6071E | ±20 mV | ±4 mV |
| AT-MIO-16E-1<br>6060E, 6061E<br>604xE | ±200 mV | ±30 mV |
| PCI-6024E<br>6025E | ±42 mV | N/A |
| DAQCard-6024E | ± 13 mV | N/A |
| 6020E<br>6021E | ±100 mV | N/A |
| 6062E | ±80 mV | ±30 mV |

Duration

| | |
|---|---|
| 607xE<br>6060E, 6061E<br>604xE | 1.5 µs |
| 6024E<br>6025E | 2 µs |
| 6020E<br>6021E<br>6062E | 3 µs |

#### Stability

Gain temperature coefficient
- External reference ..... ±25 ppm/°C

### Digital I/O

Number of channels

| | |
|---|---|
| 6021E<br>6025E | 32 input/output |
| All others | 8 input/output |

## 12-Bit E Series (NI 607xE, NI 606xE, NI 604xE, NI 602xE) (continued)

Compatibility ..... 5 V/TTL
Power-on state ..... Input; high impedance
Digital logic levels
DIO<0..7> on all devices
PA<0..7>, PB<0..7>, PC<0..7> on remaining 24 lines of 6021E and 6025E

| Level | Minimum | Maximum |
|---|---|---|
| Input low voltage | 0 V | 0.8 V |
| Input high voltage | 2 V | 5 V |
| Output low voltage ($I_{out}$ = 24 mA) | – | 0.4 V |
| Output high voltage ($I_{out}$ = 13 mA) | 4.35 V | – |

| Level | Minimum | Maximum |
|---|---|---|
| Input low voltage | 0 V | 0.8 V |
| Input high voltage | 2 V | 5 V |
| Output low voltage ($I_{out}$ = 2.5 mA) | – | 0.4 V |
| Output high voltage ($I_{out}$ = 2.5 mA) | 3.9 V | – |

Data transfers

| | |
|---|---|
| 6021E<br>6025E | Interrupts, programmed I/O |
| All others | Programmed I/O |

Handshaking (6021E and 6025E only)
Direction ..... Input or output
Modes ..... 2-wire
Transfer rate (1 word = 8 bits)
Maximum with NI-DAQ™, system dependent

| | |
|---|---|
| DAQPad-6070E | 5 kwords/s |
| All others | 50 kwords/s |

Constant sustainable rate ..... 1 to 10 kwords/s, typical

### Timing I/O

#### General-Purpose Up/Down Counter/Timers

Number of channels ..... 2
Resolution ..... 24 bits
Compatibility ..... 5 V/TTL
Digital logic levels

| Level | Minimum | Maximum |
|---|---|---|
| Input low voltage | 0 V | 0.8 V |
| Input high voltage | 2 V | 5 V |
| Output low voltage ($I_{out}$ = 5 mA) | – | 0.4 V |
| Output high voltage ($I_{out}$ = 3.5 mA) | 4.35 V | – |

Base clocks available ..... 20 MHz and 100 kHz
Base clock accuracy ..... ±0.01%
Maximum source frequency ..... 20 MHz
External source selections[1] ..... PFI0..PFI9, RTSI0..RTSI6, analog trigger; software selectable
External gate selections[1] ..... PFI0..PFI9, RTSI0..RTSI6, analog trigger; software selectable
Minimum source pulse duration ..... 10 ns
Minimum gate pulse duration ..... 10 ns, edge-detect mode
Data transfers
PCI, PXI, AT, DAQPad for IEEE 1394 ..... DMA, interrupts, programmed I/O
DAQCard, DAQPad for USB ..... Interrupts, programmed I/O
DMA modes
PCI, PXI, DAQPad for IEEE 1394 ..... Scatter-gather (single transfer, demand transfer)
AT ..... Single transfer, demand transfer

#### Frequency Scaler

Number of channels ..... 1
Resolution ..... 4 bits
Compatibility ..... 5 V/TTL
Digital logic levels

| Level | Minimum | Maximum |
|---|---|---|
| Input low voltage | 0 V | 0.8 V |
| Input high voltage | 2 V | 5 V |
| Output low voltage ($I_{out}$ = 5 mA) | – | 0.4 V |
| Output high voltage ($I_{out}$ = 3.5 mA) | 4.35 V | – |

Base clocks available ..... 10 MHz, 100 kHz
Base clock accuracy ..... ±0.01%
Data transfers ..... Programmed I/O

### Triggers

#### Analog Triggers

Number of triggers

| | |
|---|---|
| 607xE<br>606xE<br>604xE | 1 |
| 602xE | None |

Purpose
Analog input ..... Start and stop trigger, gate, clock
Analog output ..... Start trigger, gate, clock
General-purpose counter/timers ..... Source, gate
Source

| | |
|---|---|
| 6070E<br>6062E, 6060E<br>604xE,<br>602xE | ACH<0..15>, PFI0/TRIG1 |
| 6071E<br>6061E | ACH<0..63>, PFI0/TRIG1 |

Level
Internal source, ACH<0..15/63> ..... ±Full-scale
External source, PFI0/TRIG1 ..... ±10 V
Slope ..... Positive or negative; software selectable
Resolution ..... 8 bits, 1 in 256
Bandwidth (-3 dB)

| Device | Internal Source | External Source |
|---|---|---|
| 607xE | 2 MHz | 7 MHz |
| 6060E, 6061E | 1 MHz | 7 MHz |
| 6062E | 500 kHz | 2.5 MHz |
| 604xE | 2 MHz | 3 MHz |

Hysteresis ..... Programmable
Accuracy ..... ±5% of full-scale range max

#### Digital Triggers (all devices)

Number of triggers ..... 2
Purpose
Analog input ..... Start and stop trigger, gate, clock
Analog output ..... Start trigger, gate, clock
General-purpose counter/timers ..... Source, gate
Source[1] ..... PFI0..PFI9, RTSI0..RTSI6
Slope ..... Positive or negative; software selectable
Compatibility ..... 5 V/TTL
Response ..... Rising or falling edge
Pulse width ..... 10 ns minimum
External input for digital or analog trigger ... (PFI0/TRIG1)
Impedance
6062E ..... 12 kΩ
All others ..... 10 kΩ
Coupling ..... DC
Protection
Digital trigger ..... -0.5 to Vcc + 0.5 V
Analog trigger
On/off/disabled ..... ±35 V

### Calibration

Recommended warm-up time ..... 15 minutes; 30 minutes for DAQCard and DAQPad
Calibration interval ..... 1 year
Onboard calibration reference
DC level ..... 5.000 V (±3.5 mV) over full operating temperatures, actual value stored in EEPROM
Temperature coefficient ..... ±5 ppm/°C max
Long-term stability ..... ±15 ppm/$\sqrt{1000\ h}$

# E Series Multifunction DAQ Specifications

## 12-Bit E Series (NI 607xE, NI 606xE, NI 604xE, NI 602xE) (continued)

### RTSI (PCI, DAQPad-6070E for IEEE 1394, and ISA only)

Trigger lines
- PCI, ISA ..... 7
- DAQPad for IEEE 1394 ..... 4

### PXI Trigger Bus (PXI only)

- Trigger lines ..... 6
- Star trigger ..... 1

### Bus Interface

- PCI, PXI, DAQPad for IEEE 1394 ..... Master, slave
- AT, DAQCard, DAQPad for USB ..... Slave

### Power Requirements[2]

| Device | +5 VDC (±5%)* | Power Available at I/O Connector |
|---|---|---|
| 607xE | 1.1 A | +4.65 to +5.25 VDC, 1 A |
| 6060E, 6061E 6040E | 1.0 A | +4.65 to +5.25 VDC, 1 A |
| 602xE, (except DAQPad and DAQCard) | 0.7 A | +4.65 to +5.25 VDC, 1 A |
| DAQCard-6062E | 340 mA typical 750 mA maximum | +4.65 to +5.25 VDC, 250 mA |
| DAQCard-6024E | 270 mA typical 750 mA maximum | ±4.65 to +5.25 VDC, 250 mA |
| DAQCard-AI-16E-4 | 280 mA typical 400 mA maximum | +4.65 to +5.25 VDC, 250 mA |

| Device | Power | Power Available at I/O Connector |
|---|---|---|
| DAQPad-6020E | 15 W, +9 to +30 VDC | +4.65 to +5.25 VDC, 1 A |
| DAQPad-6070E | 17 W, +9 to +25 VDC | +4.65 to +5.25 VDC, 1 A |

Discharge time with BP-1 battery pack

*Excludes power consumed through I/O connector.

- IEEE 1394 DAQPads ..... 2.5 hours, typical
- USB DAQPads ..... 3 hours, typical

### Physical[2]

Dimensions (not including connectors)
- PCI[2] ..... 17.5 by 9.9 c m (6.9 by 3.9 in.)
- PXI ..... 16.0 by 10.0 c m (6.3 by 3.9 in.)
- AT (long) ..... 33.8 by 9.9 c m (13.3 by 3.9 in.)
- AT (short) ..... 17.5 by 9.9 c m (6.9 by 4.2 in.)
- DAQPad (30 cm enclosure) ..... 25.4 by 30.5 by 4.6 c m (10 by 12 by 1.8 in.)
- DAQPad (15 cm enclosure) ..... 14.6 by 21.3 by 3.8 c m (5.8 by 8.4 by 1.5 in.)
- DAQCard ..... Type II PC Card

I/O connector[2]

| | |
|---|---|
| 6070E<br>6060E<br>6040E<br>6020E<br>6023E<br>PCI-6024E | 68-pin male 0.050 D-type |
| DAQCard-6062E,<br>DAQCard-6024E | 68-pin female VHDCI |
| 6071E<br>6061E<br>6021E<br>6025E | 100-pin female 0.050 D-type |
| DAQCard-AI-16E-4 | 68-pin female PCMCIA |

### Environment

- Operating temperature ..... 0 to 55 °C; 0 to 40 °C for DAQCard-6062E and DAQCard-6024E with a maximum internal temperature of 70 °C as measured by onboard temperature sensor; case temperature should not exceed 55 °C for any DAQCard
- Storage temperature ..... -20 to 70 °C
- Relative humidity ..... 10 to 90%, noncondensing

### Certifications and Compliances

**CE Mark Compliance CE**

1 Refer to RTSI™ specifications for available RTSI trigger lines.

2 See page 184 for RT Series devices power requirements and dimensions.

## APPENDIX E

## I/O CONNECTOR BOARD FOR DAQ-AI-16E-4

This appendix describes the I/O pin assignment for the NI-DAQCard-AI-16E-4 connector board.

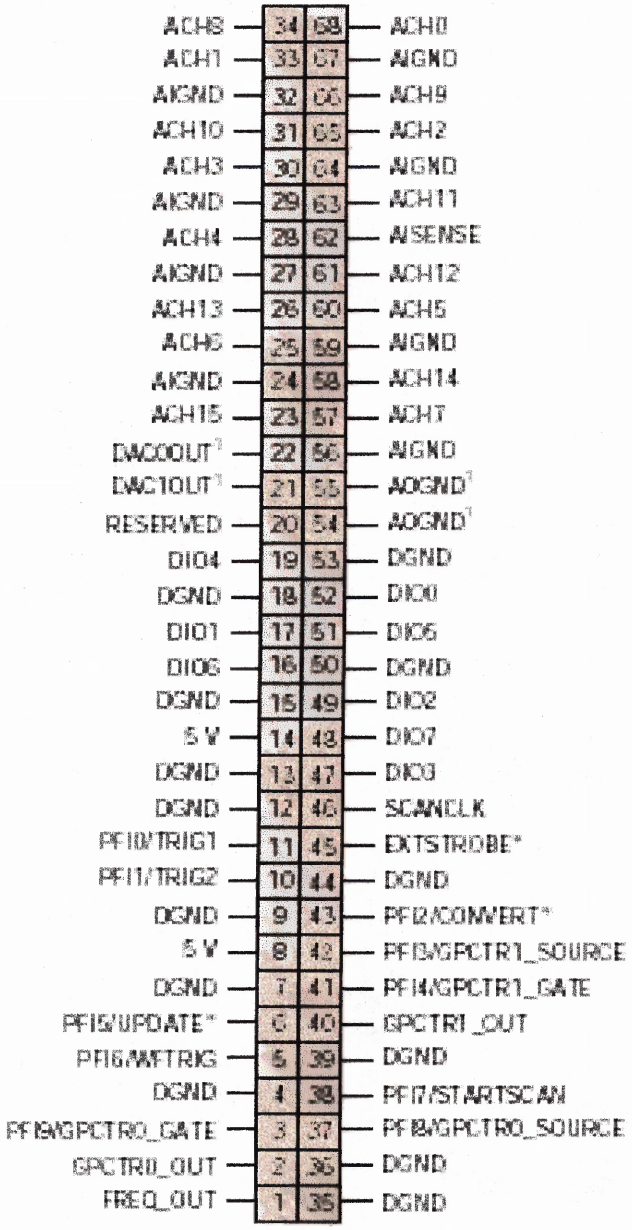

The table E.1 below shows the I/O pin assignment for the NI-DAQCard-AI-16E-4 connector board for this model.

**Table E.1** I/O Pin Assignment for the NI-DAQCard-AI-16E-4 Connector Board

| PIN FROM CB-68LP I/O CONNECTOR BLOCK | CONNECTED TO THE PHYSICAL MODEL |
|---|---|
| 16 | VALVE 2 FOR UPPER MUSCLE |
| 19 | VALVE 2 FOR LOWER MUSCLE |
| 49 | VALVE 1 FOR LOWER MUSCLE |
| 52 | VALVE 1 FOR UPPER MUSCLE |
| 18 | DIGITAL GROUND |

## APPENDIX F

## ACTIVATION OF THE SOLENOID VALVES USING MAX & LABVIEW

This appendix describes the LabVIEW program which was used for the activation of the four solenoid valves using MAX v.2.0.

Control panel of the LabVIEW program.

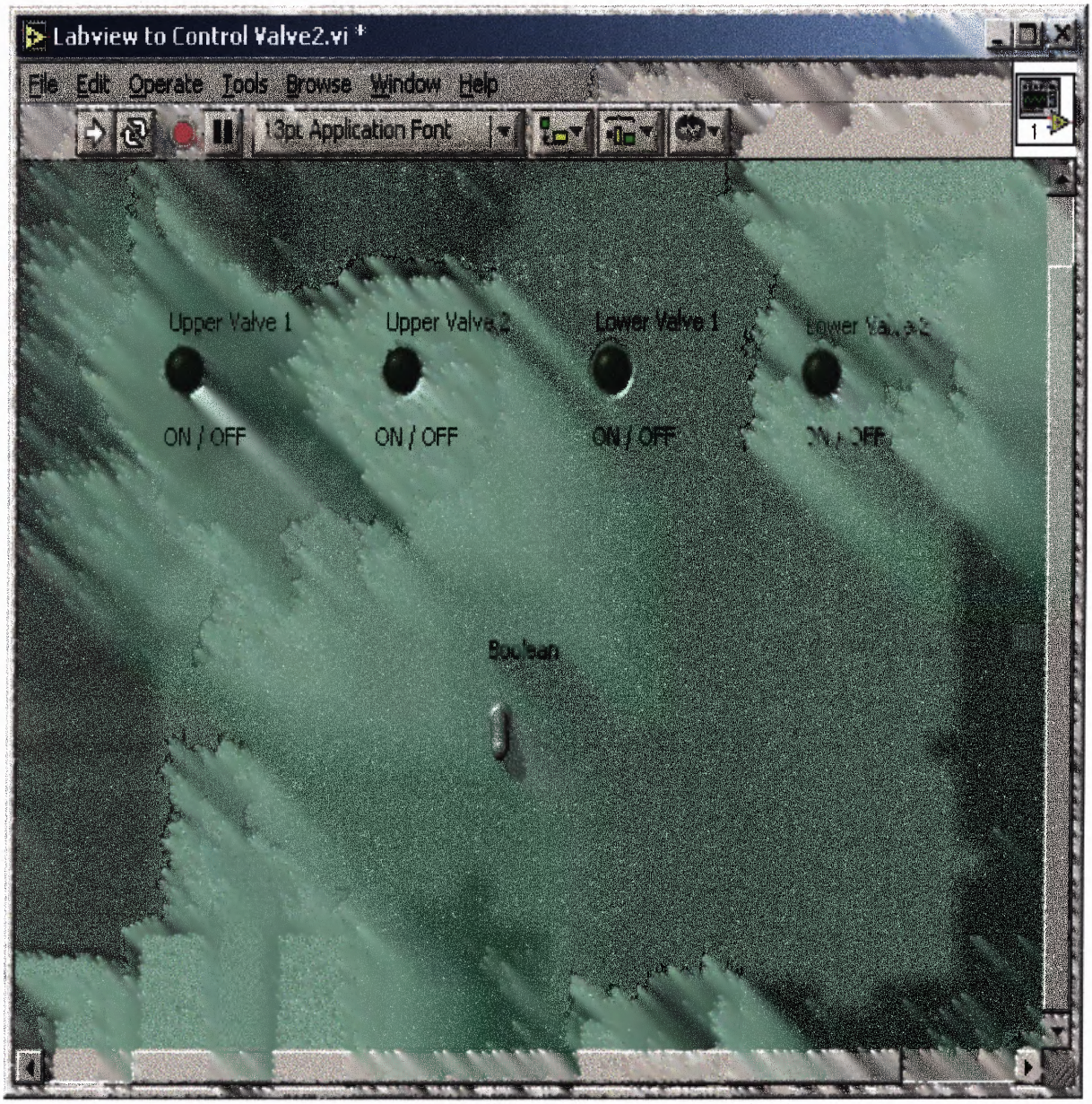

**Block Diagram of the control panel.**

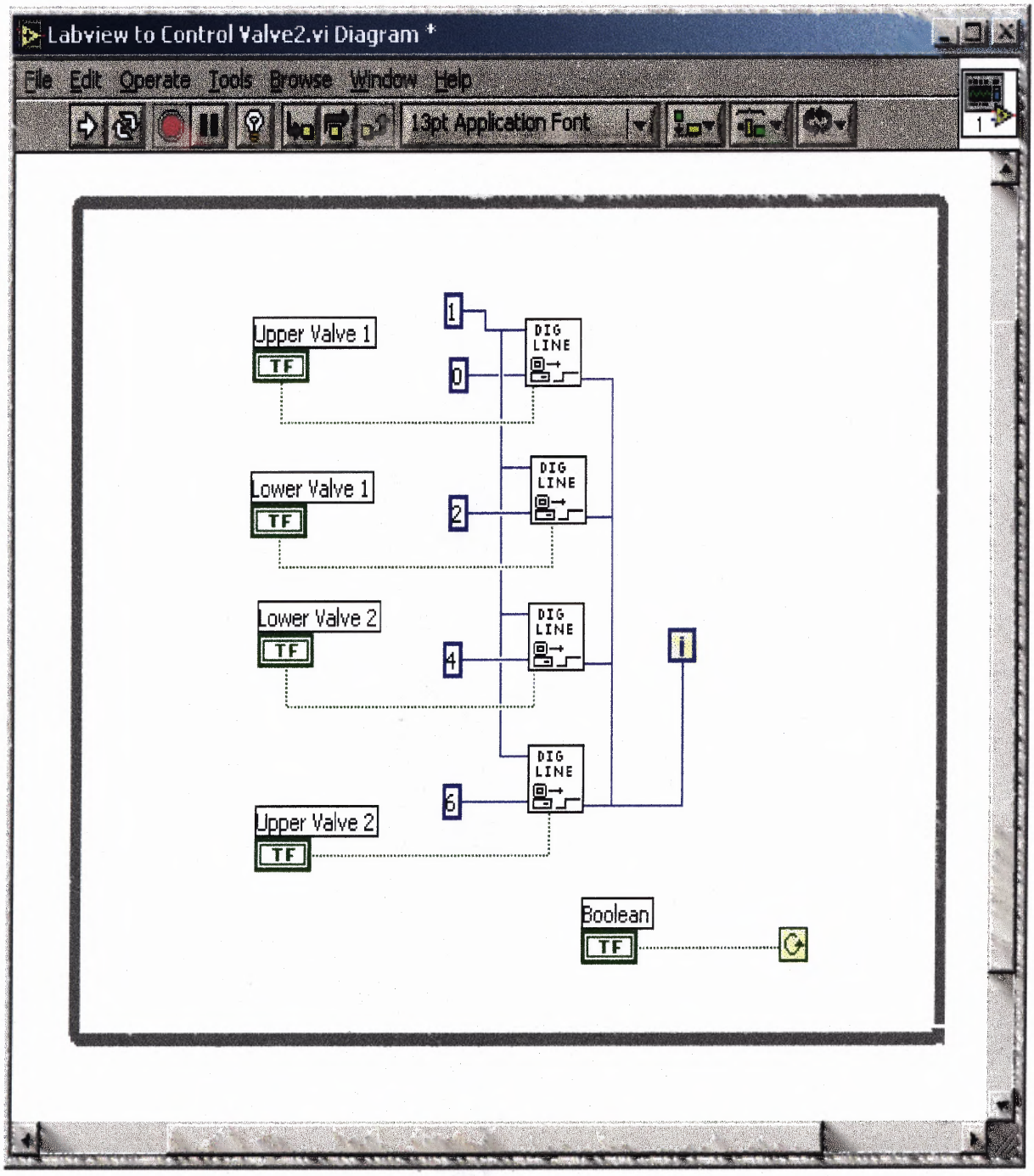

## APPENDIX G

## BANG-BANG CONTROLLER PROGRAM

This appendix describes all of the program contents and icons used in the Bang-Bang control progrm.

### Front Panel

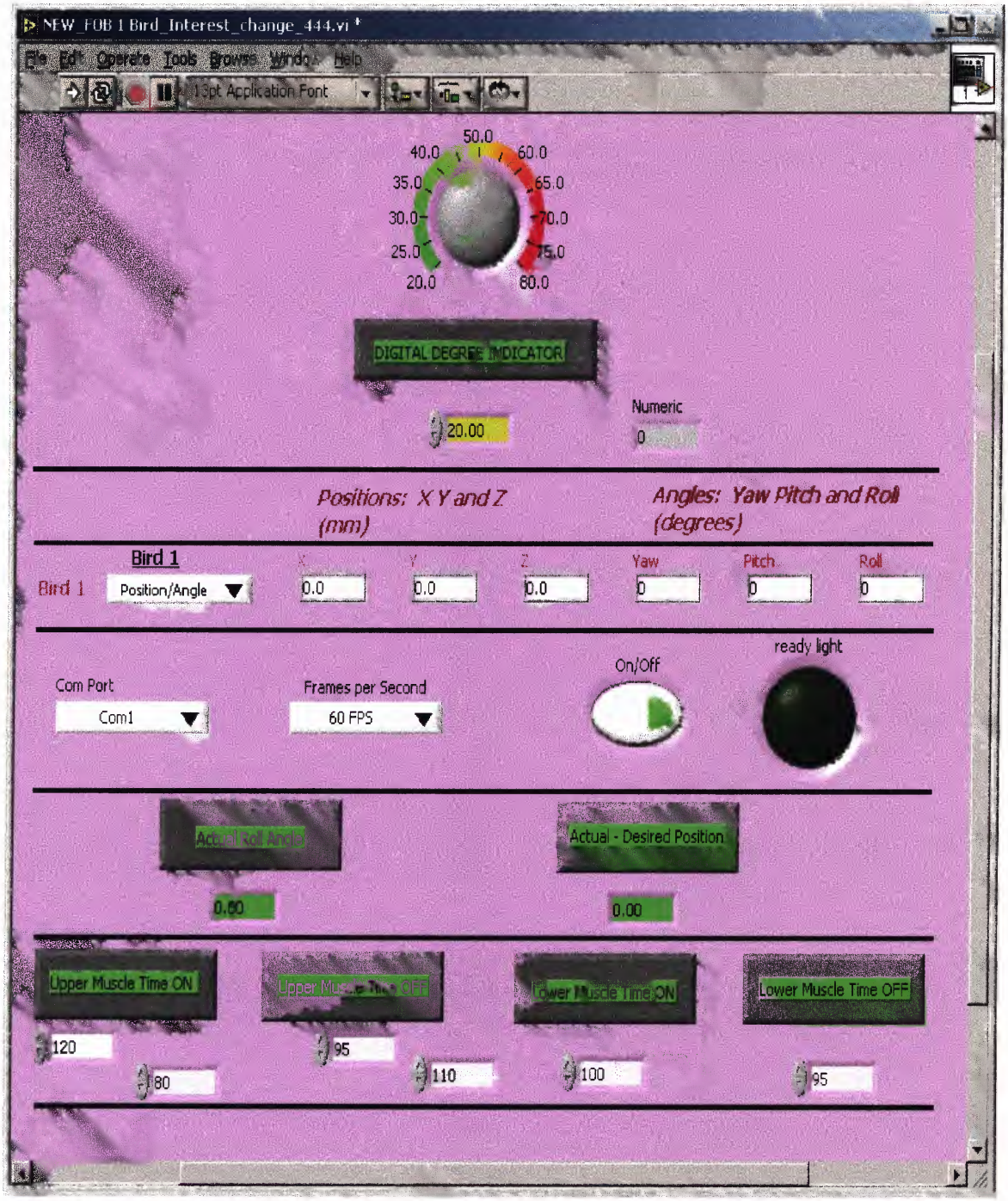

## Block Diagram 1 of 3

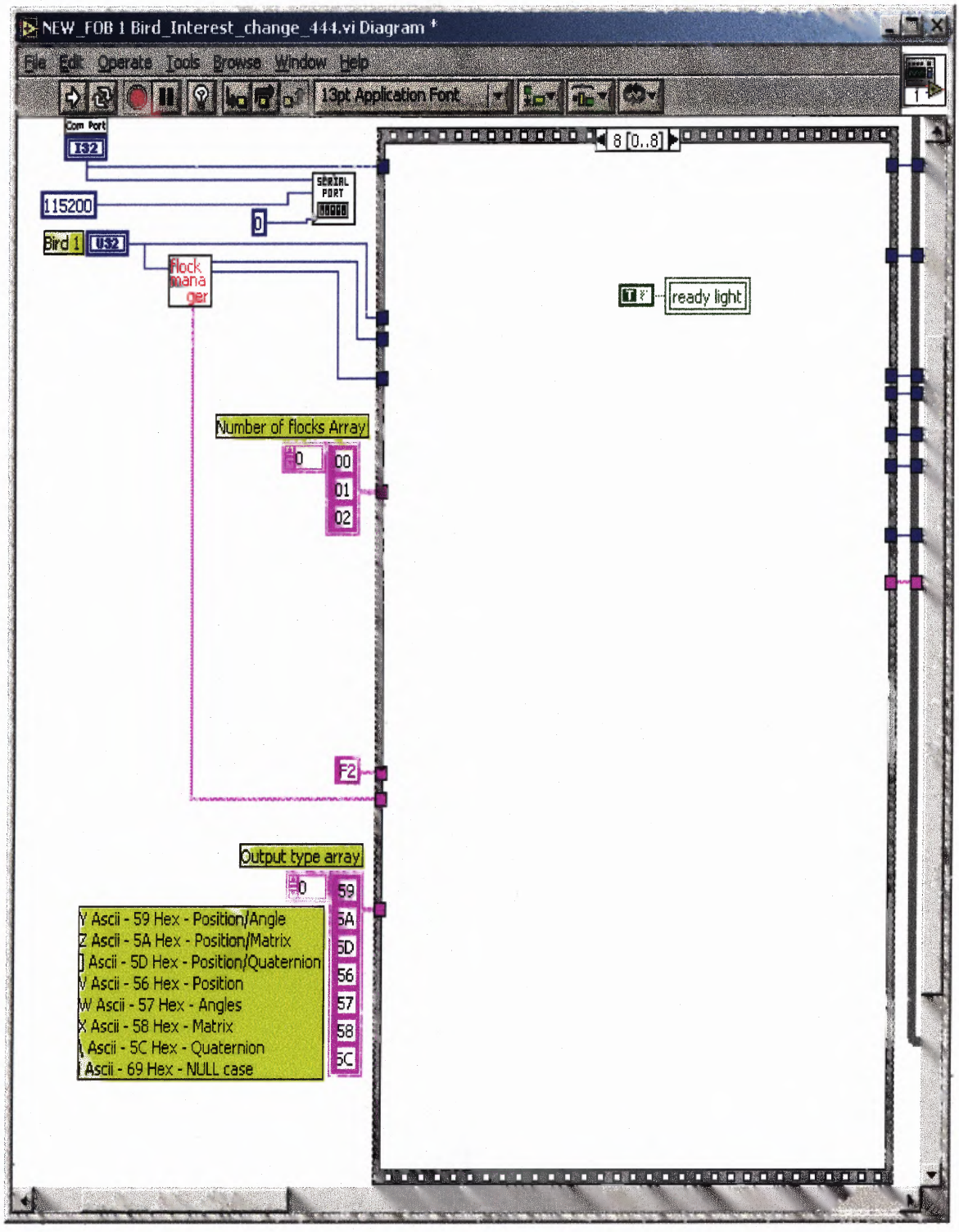

## Block Diagram 2 of 3

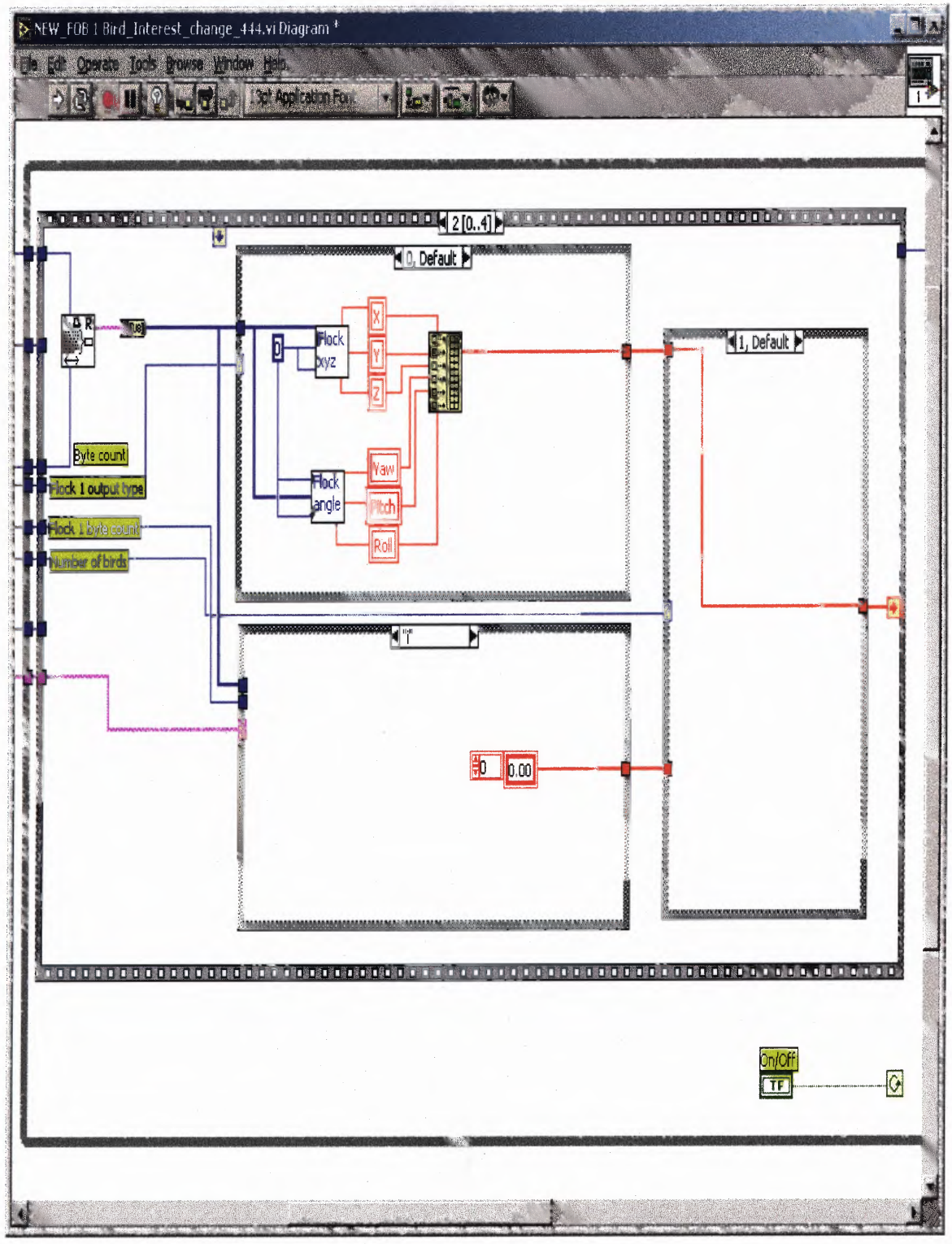

# Block Diagram 3 of 3

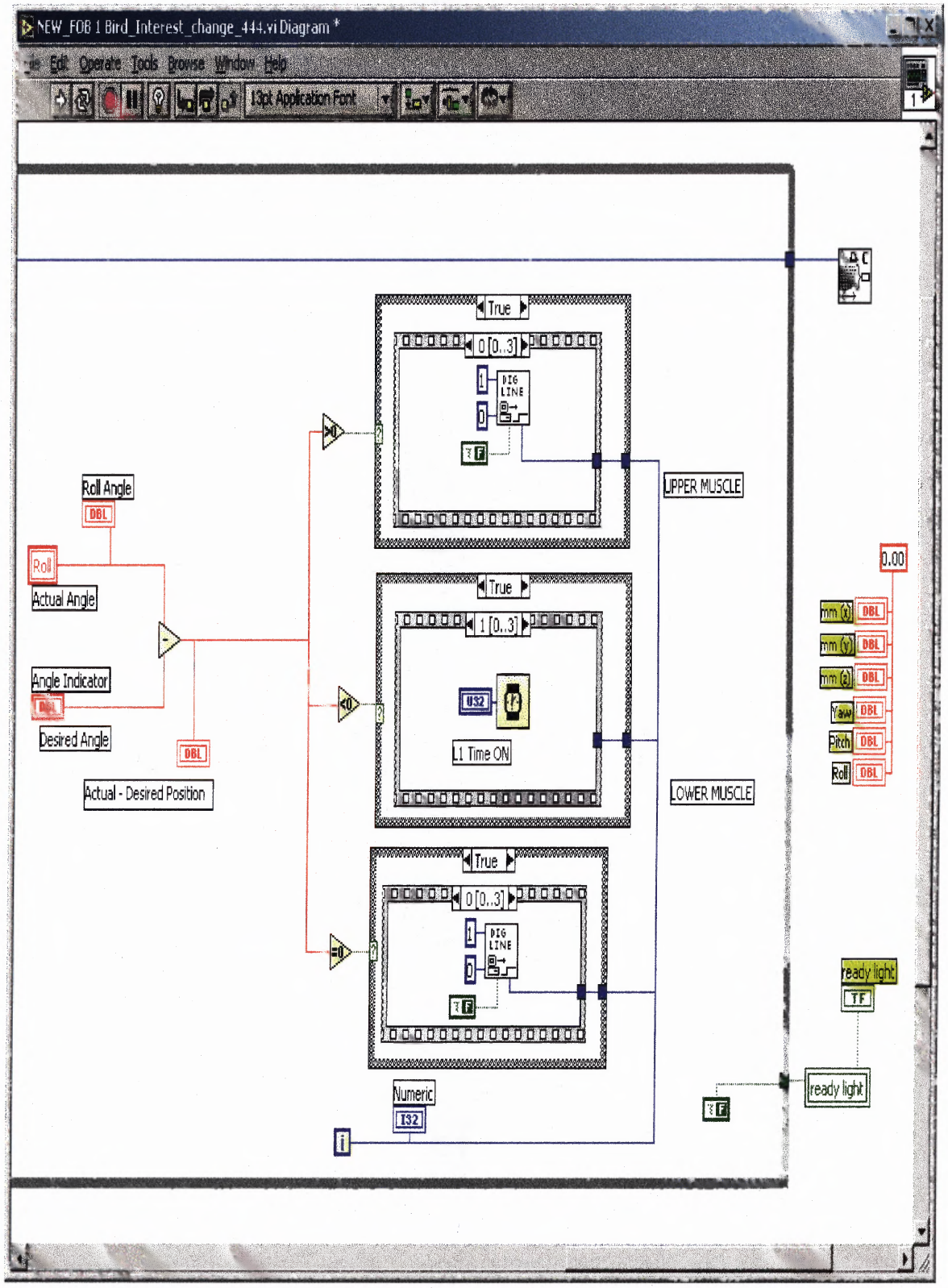

## APPENDIX H

## DIGITAL PROPORTIONAL CONTROL PROGRAM

This appendix describes the proposed program to be used in conjunction with some of the components of the original Bang-Bang control program. This program highlights the implementation of the non-linear pulse width modulated digital proportional (P) control.

### Front Panel

# Block Diagram

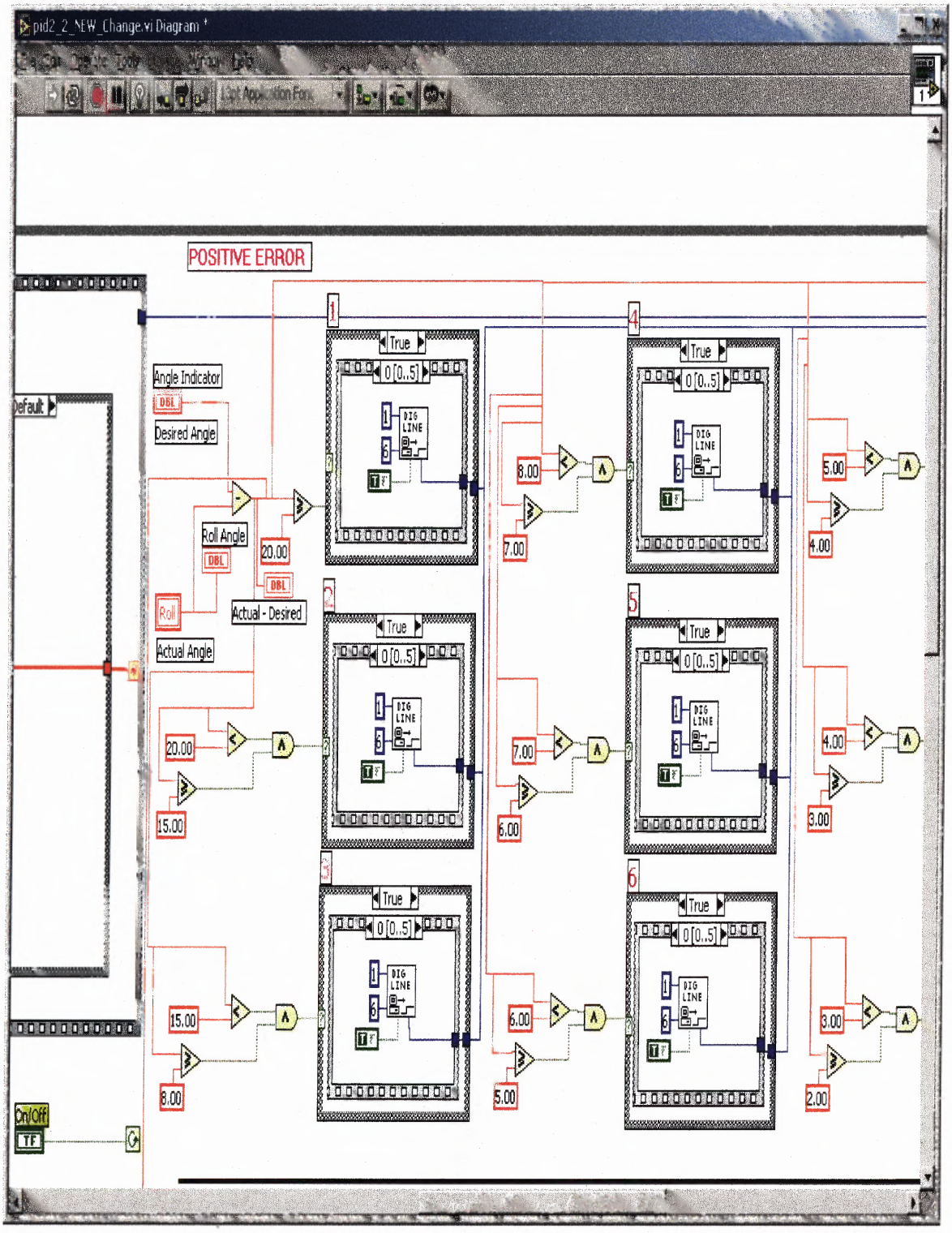

# Block Diagram

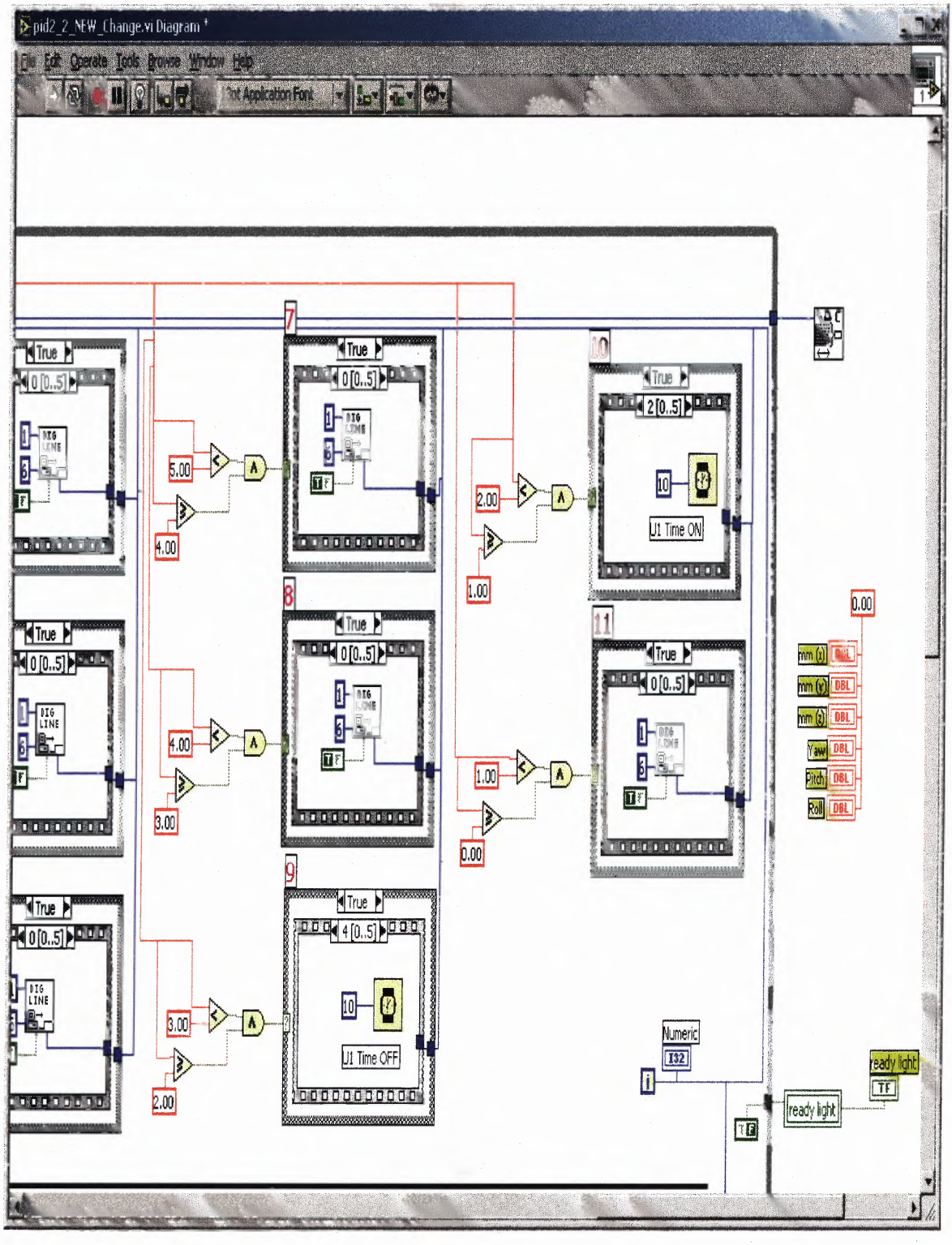

# Block Diagram

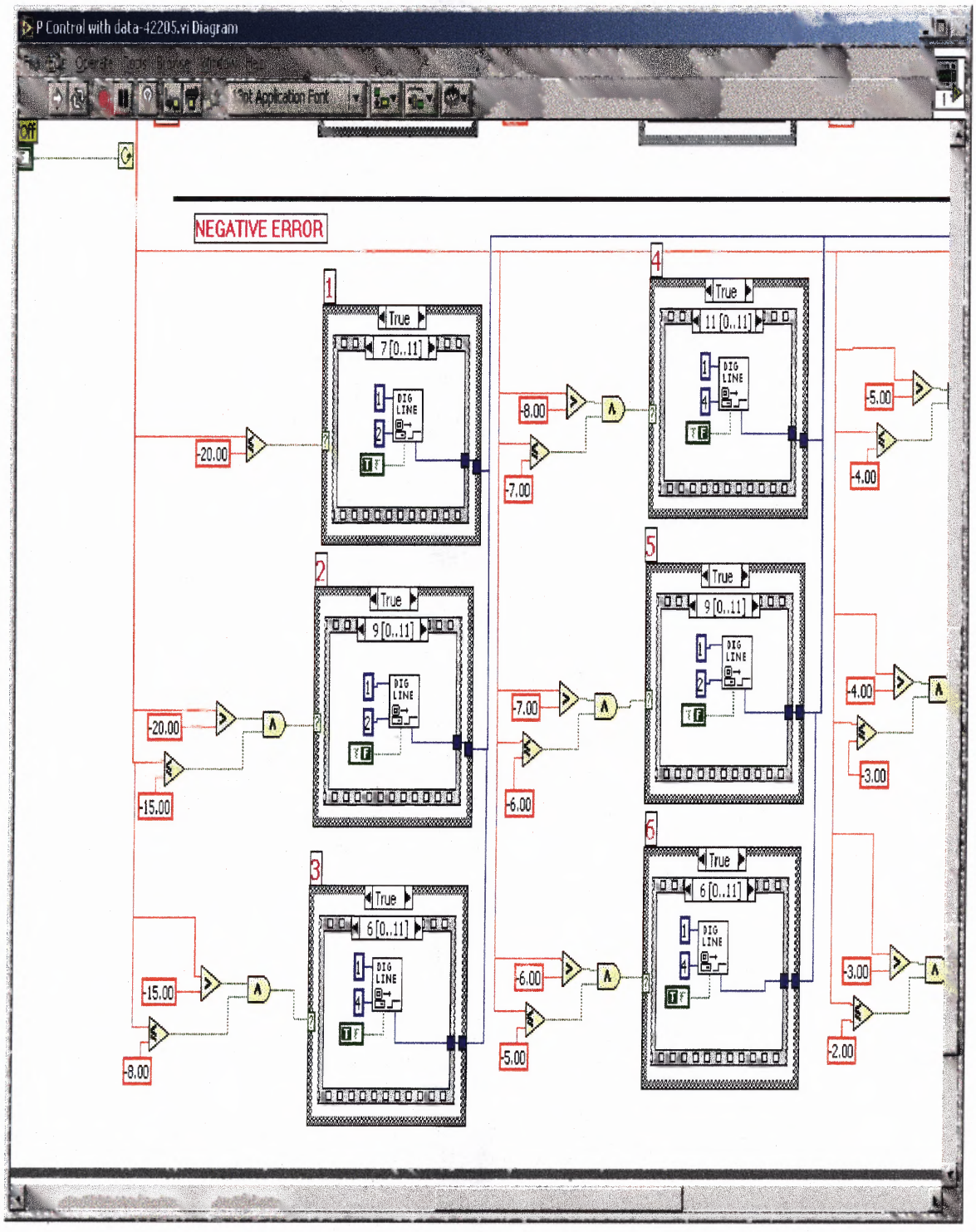

## REFERENCES


[1] Altruis BME Network, Muscles. http://www.e-muscles.net/ (10 April 2005).

[2] Van der Helm, F. C. T., Veeger, H. E. J., Pronk, G. M., Van der Woude, L. H. V. and Rozendaal, R. H. (1992). Geometry parameters for musculoskeletal modeling of the shoulder mechanism. Journal of Biomechanics, 25, 129-144.

[3] Hasan, Z. (1983). A model of spindle afferent response to muscle stretch. Journal of Neurophysiology, 49, 989-1006.

[4] Biomechanics and Motor control of Human movement, Second Edition, David A. Winter.

[5] Holmes, K. C., Wiley, Chichester (1998). The limits of Reductionism in Biology. Muscle contraction. http://www.mpimf-heidelberg.mpg.de/~holmes/muscle/ muscle1.html (11 April 2005).

[6] Cerebral Palsy. (2003) http://www.people.virginia.edu /~smb4v/tutorials/cp /index.html.

[7] Winters, J. M. (1995). An improved muscle-reflex actuator for use in large-scale neuromusculoskeletal models. Annals of Biomedical Engineering,23, 359-374.

[8] Tondu, B. and Lopez, P. (2000). Modeling and control of McKibben Artificial Muscle Robot Actuators. IEEE Control Systems Magazine, 1053, 15-38.

[9] Shadow Robot Co., Ltd. (1999). Air muscles. http://www.shadow.org.uk/ products/airmuscles.shtml (15 April 2005).

[10] Flock of Birds. (2003). http://www.ascension-tech.com/products/flockofbirds.php (15 April 2005).

[11] Flock of Birds. (2003) Ascension Technology Corporation, Installation and Operation Guide. http://www.ascension-tech.com/support/downloads.php.

[12] Satcure, Inc. (2002). Hobby Electronics Tutorial. http://www.satcure-focus.com /tutor/index.htm.

[13] Marconi ECT, Inc. (2001). Understanding the Darlington Driver Circuit. http:// www.marconiect.org/index.php (15 April 2005).

[14] Mead Fluid Dynamics, Inc. (2000). Isonic 2 & 3-way Control Valves. http://www. meadfluiddynamics.com/ (12 April 2005).

[15] Torrens, R. (2004, January). 4QD-TEC. Electronics Circuits Reference Archive PUT Complimentary Feedback Pair. http://www.4qdtec.com/putpr.html (14 April 2005).

[16] National Instruments Co., Inc. (2005). E series Multifunction DAQ. http://sine.ni.com/apps/we/nioc.vp (5 April 2005).

[17] National Instruments Co., Inc. (2005). CB-68LP, 68-pin Digital and Trigger I/O Terminal Block. http://sine.ni.com/nips/cds/view/p/lang/en/nid/1187 (9 April 2005).

[18] National Instruments Co., Inc. (2005). NI DAQCard-6024E. http://sine.ni.com /nips/cds/view/p/lang/en/nid/10969 (9 April 2005).

[19] GlobelSpec, Inc. (1999). Data Acquisition and Signal Conditioning. http://data-acquisition.globalspec.com/ (12 April 2005).

[20] Carey R. Merritt, Edward Grant, Carol A. Giuliani, Spero G. Karas. (1999). A Pneumatically Actuated Elbow Device Designed for Upper Extremity Stroke Rehabilitation.

[21] Washington University School of medicine, Center for Cerebral Palsy Spasticity. (2005). http://cerebral palsy.wustl.edu/overview.html (5 April 2005).

[22] University of Exeter (2005). http://newton.ex.ac.uk/teaching/CDHW/Feedback /ControlTypes.html (10 April 2005).

[23] Richard Paradiso (2003). A Biologically Inspired Joint Model Using Engineering Methods to Enhance Understanding of Muscle Activity (Master's Thesis, New Jersey Institute of Technology, Newark, New Jersey), [on line]. Available: http://www.library.njit.edu/etd/2000s/2003/njit-etd2003-098/njit-etd2003-098.html (23 August 2003).